Fundamental Measurements on an Aggregated Dye Liquid Crystal

Viva R. Horowitz

March 15, 2005

Abstract

The nematic liquid crystal phase is a phase of matter in which the particles have a preferred orientational direction, as opposed to the liquid phase, with no preferred direction, and the solid crystal phase, with an ordered lattice structure. In an aggregated dye, or chromonic, liquid crystal, molecules come together in aggregates, and these aggregates form a liquid crystal. Aggregated dyes that form liquid crystals have been known for some time, but few fundamental measurements have been taken prior to this research. Unlike most liquid crystals, aggregated dye liquid crystals are water-soluble, opening the door to applications of liquid crystals in the fields of biology and medicine. In order to move ahead with explorations of applications and general understanding of chromonic liquid crystals, more must be known about the properties of this phase; thus, this research focuses on one aggregated dye liquid crystal, aqueous Sunset Yellow FCF. Phase diagram measurements, birefringence measurements, and order parameter measurements were obtained for aqueous Sunset Yellow. A general model of the aggregation consistent with both the results of the birefringence measurements and the results of the order parameter measurements is suggested in which the nitrogen-nitrogen double bonds of the Sunset Yellow molecule are perpendicular to the long axis of the aggregate.

Contents

List of Figures

Chapter 1

Introduction

This investigation delves into understanding an aggregated dye liquid crystal, a material that forms a liquid crystal at high concentrations due to the interactions between molecules that cause the molecules to aggregate. Measuring some fundamental properties of the liquid crystal, the phase diagram, the birefringence, and the order parameter, the research reported here has shed light on the nature of both the aggregation of the molecules and the nematic liquid crystal phase that the aggregates form.

1.1 Liquid Crystals

The liquid crystal phase of matter interests researchers for many reasons, mostly involving optical properties not seen in other fluids along with a sensitivity to external conditions. These properties have made liquid crystals useful particularly in display devices. Despite the importance of liquid crystals, there are still areas of liquid crystal science in which fundamental properties have not been measured. One example of this are the liquid crystal phases formed by aggregated dyes.

In general, the solid crystal phase of a material exhibits more order than the liquid phase. A liquid is isotropic. It has no orientational order and is therefore the same in every direction, with no preferred direction; the particles' motion is random. A solid crystal has an orientation and position for each particle, with motion generally confined to lattice vibrations. Some materials have a liquid crystal phase, in which the material is a fluid with orientational order. This has order in between the higher order of a solid crystal and the disorder of its liquid phase. Fluidity allows the liquid crystal to easily change in response to a stimulus while orientational order gives liquid crystals interesting optical properties as compared to an isotropic liquid. Only certain materials have the liquid crystal phase; the material's particles must be anisotropic, meaning that the particles are not the same in every

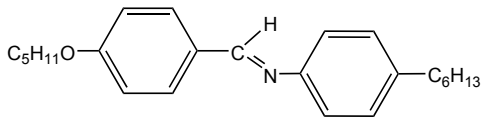

Figure 1.1: A typical calamitic, or rod-like, liquid crystal molecule [1]. This molecule forms a thermotropic liquid crystal, which needs no solvent to have a liquid crystal phase.

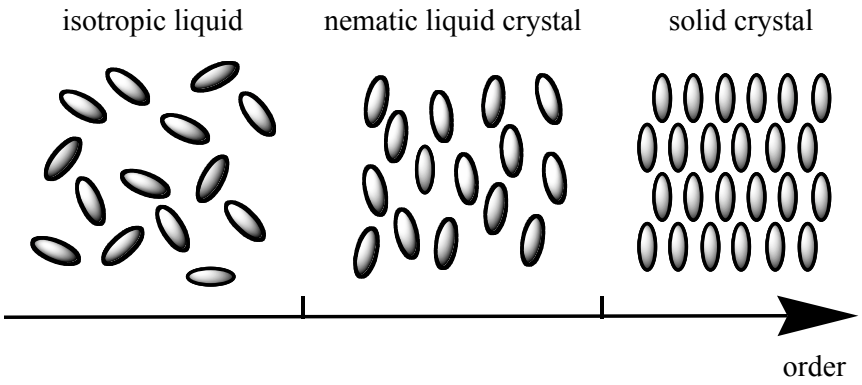

Figure 1.2: The isotropic liquid, the nematic liquid crystal, and the solid crystal are three distinct phases of matter. The liquid has no order, and is said to be isotropic because there is no preferred direction. The nematic liquid crystal distinguishes itself from other phases with orientational order in one dimension but no positional order. The solid crystal has both orientational and positional order in three dimensions, with the particles held in a lattice. In this figure, the director of the nematic liquid crystal, indicating the average direction of the particles, is vertical.

direction. In general, the particles are either rod-shaped or disk-shaped. In the former case, the liquid crystal is called calamitic; in the latter it is called discotic. Figure 1.1 shows a typical calamitic liquid crystal molecule. Figure 1.2 shows how rod-like particles form a nematic liquid crystal. In the nematic liquid crystal phase, the particles tend to line up in a particular direction, called the director, so the particles have orientational order but no positional order.

Liquid crystals are generally classified either as lyotropic liquid crystals or as thermotropic liquid crystals. Lyotropic liquid crystals emerge in solutions of compounds, and usually have a liquid crystal phase only when in solution with some solvent, with the phase depending on both temperature and concentration. In contrast, thermotropic liquid crystals have temperature-driven phase transitions, without the need for a solvent.

Most lyotropic liquid crystals have molecules with a rigid polar 'head' group and a flexible nonpolar 'tail' group, as shown in Fig. 1.3. The polar head is hydrophilic while the nonpolar tail is hydrophobic, so that at certain temperatures and concentration, the

Figure 1.3: A typical lyotropic molecule, with a polar head and a nonpolar tail.

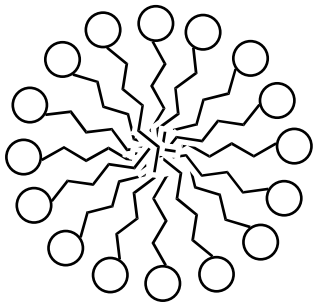

Figure 1.4: A micelle shown in cross-section. The hydrophilic heads of a lyotropic molecule aggregate to shield the hydrophobic tails of the molecule from the surrounding water. This is a liquid crystal structure typical of soap molecules.

molecules arrange into structures such as micelles, as shown in Fig. 1.4. Soaps and various phospholipids are examples of lyotropic liquid crystals with polar heads and nonpolar tails [1].

Like many solids, liquid crystals have more than one index of refraction. The index of refraction of a material is defined by $n \equiv c/v$, where c is the speed of light in the vacuum and v is the speed of light in the material. In a liquid crystal, light polarized parallel to the director experiences one index of refraction, the extraordinary index n_e, and light polarized perpendicular to the director experiences another index of refraction, the ordinary index n_o. Light polarized at some other angle with respect to the director, on the other hand, experiences more than one index of refraction. The parallel component experiences the extraordinary index n_e and the perpendicular component experiences the ordinary index n_o, such that linearly polarized light becomes elliptically polarized when it passes through a liquid crystal. This results in the optical property of birefringence, or double refraction, illustrated in Fig. 1.5, in which a material has two indices of refraction, n_e and n_o.

In addition to the birefringence, a second measurable property, the order parameter, reveals the structure of the material, in this case measuring how close the molecules are, on average, from being aligned with the director. The order parameter S will be defined in Eq. (2.17) such that an order parameter of zero corresponds to randomly oriented molecules, an order parameter of 1 corresponds to every molecule aligning with the director, and an order parameter of $-\frac{1}{2}$ corresponds to every molecule aligning perpendicular to the director.

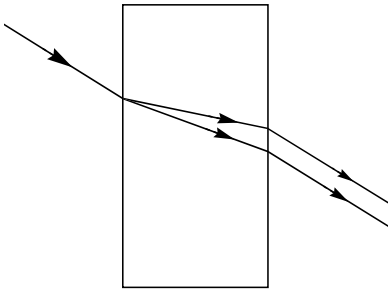

Figure 1.5: A birefringent material has two indices of refraction. One index, n_e, called the extraordinary index, is for the component of light polarized in the direction of the optical axis of the material, and the other index, n_o, the ordinary index, is for light polarized in any direction perpendicular to the optical axis. The birefringence is the difference between these two indices, $\Delta n \equiv n_e - n_o$. Some solids are birefringent and some are not. The orientational order of liquid crystals creates an anisotropy that makes liquid crystals birefringent.

1.2 Lyotropic Chromonic Liquid Crystals

Lyotropic chromonic liquid crystals form a liquid crystal phase in the aggregate, which distinguishes them from thermotropic liquid crystals. In most of the liquid crystals that have been studied, including the lyotropic liquid crystal described above, the particles that form the liquid crystal phase are molecules. However, the particles in lyotropic chromonic liquid crystals, or LCLCs, are aggregates of molecules. Though these particles are formed from multiple molecules, they exhibit a nematic liquid crystal phase nonetheless. We use the term aggregated dye liquid crystal to refer to the class of dyes that form LCLCs. In addition to dyes, certain materials used as drugs, nucleic acids, antibiotics, and anti-cancer agents have been found to have the LCLC phase [2].

Chromonic liquid crystals are considered lyotropic because they have a liquid crystal phase only while in solution. However, they differ from other lyotropic liquid crystals in a number of ways. Chromonic molecules have a different shape than the typical lyotropic molecule shown in Fig. 1.3, tending to be plank-like or disk-like. Chromonic molecules generally are rigid, without a flexible tail, and are aromatic rather than aliphatic [3], referring to parts of molecules with benzene rings. Both soap-like lyotropic molecules and LCLCs aggregate, but LCLCs have hydrophobic surfaces such that they tend to form linear aggregates in water. Soap-like molecules will aggregate until they form a micelle, at which point the lyotropic molecules have minimized their free energy, whereas in a LCLC system there is no optimum aggregate size [4]. As will be shown in section 2.1.1, the interplay between energy and entropy results in an equilibrium distribution of aggregate sizes. Figure 1.6 shows how the aggregate grows with increasing concentration and forms a nematic liquid crystal.

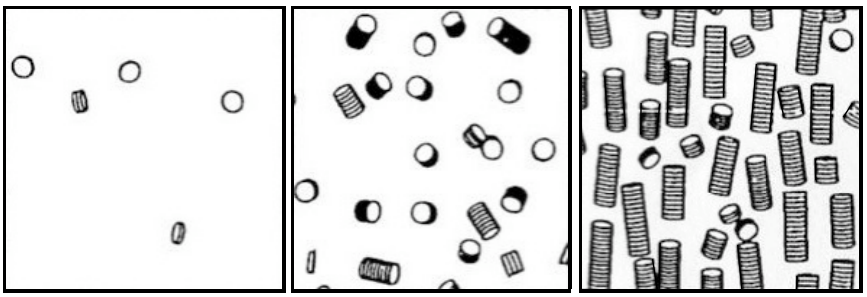

(a) mostly monomers (b) growth of aggregate (c) nematic

Figure 1.6: In some cases, the particles forming a liquid crystal are aggregates of molecules rather than single molecules. Here we see an LCLC at various concentrations. At low concentrations (a), the molecules are mostly monomers with some dimers, and the substance is in the liquid phase. As the concentration increases (b), the aggregates grow until (c) they form particles that show a preferred direction, and the substance is in the liquid crystal phase. There are two levels of structure. On the smaller level, molecules aggregate together as the concentration increases. On the larger level rod-like particles made up of aggregated molecules form a nematic liquid crystal phase. From Ref. [5].

Comparing Fig. 1.6 with Fig. 1.2 shows that the chromonic nematic liquid crystal phase is more similar to the thermotropic nematic liquid crystal phase than to the micelle shown in Fig. 1.4, as noted by Ref. [2]. Although both chromonics and micelle-forming lyotropics are considered lyotropic liquid crystals, chromonics have much in common structurally with thermotropic liquid crystals.

1.3 Prior Work in this Area

LCLCs were occasionally observed but were a mystery until 1971, when the first basic observations and phase diagram of one LCLC were published. Most prior work in the area of chromonic liquid crystals has been in classifying the phases of chromonic liquid crystals, including the nematic (N), and hexagonal columnar (M) phases. Cox et al. [6] observed the phases of the LCLC drug disodium chromoglycate (DSCG) and plotted a phase diagram in 1971 [4, 7], and soon thereafter, negative birefringence was observed in the nematic phase of DSCG [7]. DSCG is very water soluble and, according to optical microscopy observations, has two mesophases, the N phase and the M phase [4]. The M phase is thought to be a positionally ordered phase in which the columns are ordered in a two dimensional hexagonal pattern. X-ray diffraction studies show a peak at 0.34 nm for DSCG [6–8]; this is the spacing between molecules of DSCG in the aggregate [4]. NMR measurements of DSCG show that

the order parameter is quite high [8]. The order parameter of bonds in DSCG, based on absorption measurements, is negative, and equal to values around -0.1, depending on the bond measured [9]. Other studies of DSCG include sodium NMR spectra [10]. More LCLCs were discovered and measured [11], until it became apparent that lyotropic chromonic liquid crystal systems like DSCG are common [12].

Other than studies of DSCG, many of the studies of LCLCs have been qualitative. In addition, some quantitative measurements have been taken, including NMR and X-ray measurements of 7,7'-DSCG [13] and of some xanthone derivatives [14]. Many measurements are aimed at understanding the underlying structures of LCLCs. Polarizing optical microscopy and X-ray diffraction measurements of a cyanine dye and of C.I. Acid Red 266 suggest that C.I. Acid Red 266 aggregates in a hollow tube structure, cyanine dye molecules aggregate in a brickwork structure [15], and the azo dye C.I. Direct Blue has unimolecular stacking [16]. The aggregate columns of a dye LCLC, Violet 20, was imaged at high magnification by atomic force microscopy, showing columns generally 1-2 nm in width and 1-2 nm apart [17]. The 0.34 nm stacking separation between molecules, independent of concentration and temperature, seems to be common in LCLC systems [4, 16]. Stegemeyer and Stöckel measured the average number of molecules within an aggregate of pseudo isocyanine chloride to be in the range of 40 to 50, measured spectroscopically near the isotropic-nematic transition [18]. These studies show that in general, LCLC systems have both a nematic and a columnar phase and that the stacking distance between molecules is generally 0.34 nm.

What causes LCLC molecules to aggregate? In general, the flat molecules pack face-to-face to form a molecular stack. This packing is called the π-π interaction. Lydon [2] notes that there are two ideas for why chromonic molecules aggregate in water. The first is that molecules are simply avoiding the water. The aromatic rings generally found in the center of these flat molecules are not water soluble, and so by stacking together, the aromatic rings have less contact with the water. The second idea is that the conventional van der Waals' forces from atom center to atom center explain stacking. Maiti et al. [3] have shown that computer simulations of hydrophobic molecules with small hydrophilic peripheries exhibit columnar aggregation of the molecules. They modeled each molecule of an LCLC as a diamond pattern of seven touching hydrophobic spheres with hydrophilic spheres at each end, and found that for aggregation to take place it is necessary that the molecule have an overall hydrophobicity.

Some current research explores applications of LCLCs. Ichimura et al. [19] studied photoalignment of dye LCLCs, with potential applications to stereoscopic liquid crystal displays. Shiyanovskii et al. [20] have proposed a microbial sensor that uses DSCG to detect and amplify the presence of immune complexes.

Turner's dissertation reported that Sunset Yellow FCF has a liquid crystal phase [11], and Luoma's dissertation investigated this phase of Sunset Yellow using optical, magnetic, and X-ray techniques [5], finding that the stacking distance is again 0.34 nm. In the research reported here, the investigation of the nematic phase of Sunset Yellow is continued with optical measurements.

1.4 Motivation and Goals

Compared to other liquid crystals, very little is known about the molecular interactions or the phase of LCLCs, with the exception of DSCG. There is a great deal of data for DSCG, but only a general understanding of other LCLCs has been established. Clearly, there is plenty more to explore in this field. In order to better understand the structure of LCLCs, I studied the optical properties of one LCLC, Sunset Yellow FCF. Sunset Yellow was chosen as a representative of the many aggregated dye liquid crystals known to exist. I plotted a phase diagram, measured the birefringence of various concentrations of solution, and measured the order parameter of Sunset Yellow. Based on these optical measurements, I suggested a model of the aggregate.

1.5 Organization

Chapter 2 discusses the statistical mechanics of the aggregation; the form of the phase diagram is predicted by making assumptions about the entropy, energy, and interactions of the molecules and aggregates. Following this, a discussion of the anisotropy and optics of liquid crystals leads to a formula for measuring the order parameter. Chapter 3 describes Sunset Yellow FCF, the aggregated dye liquid crystal studied here. Chapter 4 describes the procedure used in collecting data for the phase diagram, the birefringence, and the order parameter of the liquid crystal. This includes Jones calculations showing how the experimental setup for the birefringence measurements made it possible to arrive at the birefringence. Chapter 5 presents four graphs of data collected: the phase diagram, birefringence measurements, the index of refraction of isotropic Sunset Yellow, and the order parameter of a sample of Sunset Yellow. Chapter 6 presents a general model of the aggregation of Sunset Yellow, compares the theoretical and experimental phase diagrams, and compares the work of others to results presented here. Chapter 7 concludes the thesis.

Chapter 2

Theory

2.1 Statistical Mechanics of Aggregation

The temperature and the concentration of Sunset Yellow determine the size of its aggregates and its phase. Here we use the statistical mechanics of aggregation and, in section 2.1.2, the mechanics of nematic liquid crystal particles, to predict the size distribution of the aggregates and the phase of the solution.

2.1.1 Finding the Number of Molecules in the Aggregate

We will determine the average expected length $\langle n \rangle$ of the aggregate by minimizing the Helmholtz free energy F of the system of aggregates.

It is useful to define a number of constants and variables.

$$
\begin{aligned}
F &= \text{the Helmholtz free energy of the system,} \\
E &= \text{the energy of the system of aggregates,} \\
T &= \text{the temperature,} \\
S &= \text{the entropy of the system,} \\
i &= \text{the number of molecules in an aggregate,} \\
\epsilon &= \text{the energy gained each time two molecules aggregate,} \\
N &= \text{the number of aggregates in the solution} \\
N_i &= \text{the number of aggregates of length } i \text{ in the solution,} \\
V &= \text{the volume,} \\
\nu_i &= N_i/V = \text{the number of aggregates of length } i \text{ per unit volume,} \\
k_B &= \text{Boltzmann's constant} = 1.38065 \times 10^{-23} \text{ J/K,}
\end{aligned}
$$

$$
\begin{aligned}
h &= \text{Planck's constant} = 6.62607 \times 10^{-34}\ \mathrm{m^2\,kg/s}, \\
b_1 &= \text{the volume of one molecule in the aggregate}, \\
\Phi &= \text{the volume fraction of the sample in water} \\
M_w &= \text{the molecular weight, and} \\
\langle n \rangle &= \text{the average number of molecules in an aggregate.}
\end{aligned}
$$

The following calculation of the free energy F and of the the number of aggregates of length i per unit volume ν_i follows a similar calculation Ref. [5, pp. 31-32] for the aggregation of DSCG.

The mass of a single molecule in the aggregate is ρb_1, where ρ is the mass density of aggregated Sunset Yellow.[1] Then $m_i = i\rho b_1$ is the mass of an aggregate of i molecules.

For Sunset Yellow FCF, some values are known. The molecular weight is $M_w = 0.45238$ kg/mol. We know the area of a molecule of Sunset Yellow by computer model[2]. Multiplying this area by the stacking separation measured by Ref. [5], 0.34 nm, we find that the volume of a molecule of Sunset Yellow in the aggregate is $b_1 = 4.5 \times 10^{-28}$ m^3. We assume that the system is isodesmic, i.e., that the energy gained when two molecules of Sunset Yellow aggregate together ϵ is constant [2]. From Ref. [22], this energy is $\epsilon = 8.67 \times 10^{-20}$ J. From Ref. [5], the density of aggregated Sunset Yellow is $\rho = 1400$ kg/m^3.

We wish to find the Helmholtz free energy per unit volume F/V, where

$$F \equiv E - TS. \tag{2.1}$$

In order to calculate the free energy, we will be making a number of assumptions about the energy and entropy of the sample. The assumptions that the sample is similar to an ideal gas should only hold at low concentrations and temperatures, when the particles interact with each other less. Even if the theory breaks down at higher concentrations and temperatures, it illustrates that the basic aggregation behavior can be predicted with a very simple model.

We assume the solution of aggregates is sufficiently dilute that each aggregate is non-interacting with the other aggregates, so that the system has an entropy like that of an ideal gas. Then the Sakur-Tetrode equation [23, p. 362] gives the entropy as

$$S = Nk_B \left(\ln \frac{V}{N} + \frac{3}{2} \ln T + \frac{3}{2} \ln \frac{2\pi m k_B}{h^2} + \frac{5}{2} \right).$$

[1] An alternative approach to calculating the mass of a molecule is to use the molecular weight. However, it is unclear whether the sodium atoms should be considered a contributing component of the molecule's mass, since the sodium will tend to disassociate in water.

[2] The CAChe Scientific Molecular Modeling program, from Ref. [21].

Let Λ_i be the thermal wavelength of an aggregate of i molecules, given by

$$\Lambda_i = h \Big/ \sqrt{2\pi m_i k_B T}. \tag{2.2}$$

Then the entropy of all aggregates of i molecules is

$$S_i = V\nu_i k_B \left(\ln \frac{1}{\nu_i} + \ln T^{3/2} + \ln(T\Lambda_i^2)^{-3/2} + \frac{5}{2} \right)$$

so that the entropy per unit volume of all aggregates of i molecules is

$$\frac{S_i}{V} = -\nu_i k_B \left(\ln \nu_i \Lambda_i^3 - \frac{5}{2} \right). \tag{2.3}$$

The energy of an ideal gas is entirely kinetic, and equal to $\frac{3}{2}Nk_BT$, by the equipartition theorem [23]. However, unlike an ideal gas each aggregate has an internal energy because there is an energy ϵ gained each time two molecules aggregate. To form an aggregate of i molecules, two molecules must aggregate together $i-1$ times, so the internal energy of each aggregate is $-(i-1)\epsilon$. Note that the energy of a shorter aggregate is higher than the energy of a longer aggregate. Then the internal energy of all aggregates of i molecules per unit volume is $-\nu_i(i-1)\epsilon$. Adding the internal energy per unit volume to the energy per unit volume of an ideal gas, we arrive at the energy of the system of aggregates.

$$\frac{E_i}{V} = \frac{3}{2}\nu_i k_B T - \nu_i(i-1)\epsilon. \tag{2.4}$$

From equations (2.4) and (2.3), Eq. (2.1) gives the free energy per unit volume as

$$\frac{F}{V} = k_B T \sum_{i=1}^{\infty} \left(\nu_i \left[\ln(\nu_i \Lambda_i^3) - 1 \right] - \nu_i (i-1) \frac{\epsilon}{k_B T} \right) \tag{2.5}$$

where we sum over all aggregate lengths to calculate the total free energy. This system is in contact with a temperature reservoir, namely the heating stage, so the Helmholtz free energy is a minimum at equilibrium. Hence longer aggregates are energetically favorable but decrease the entropy, giving an equilibrium distribution of aggregate sizes. Since the system has a fixed number of solvent and dye molecules, $N_{\text{dye molecules}}/V = \sum i\nu_i$, we wish to minimize F/V subject to the constraint

$$\Phi = b_1 \sum_{i=1}^{\infty} i\nu_i = \text{constant} \tag{2.6}$$

to find the equilibrium distribution of aggregate sizes. The volume fraction Φ is the ratio of the volume of Sunset Yellow to the volume of the solution of water and Sunset Yellow. The average number of molecules in an aggregate $\langle n \rangle$ can be obtained from

$$\langle n \rangle = \frac{N_{\text{dye molecules}}/V}{N_{\text{aggregates}}/V} = \frac{\sum i\nu_i}{\sum \nu_i} = \frac{\Phi}{b_1 \sum \nu_i} \tag{2.7}$$

where the sums are over i.

Let λ be a Lagrange multiplier and let

$$\mathcal{F}_i \equiv \frac{F_i}{V k_B T} + \lambda \Phi$$

where F_i/V is the free energy per unit volume of all aggregates of i molecules. The free energy is minimized when the partial derivative of $\mathcal{F}_i$ vanishes,

$$\frac{\partial \mathcal{F}_i}{\partial \nu_i} = \frac{\partial}{\partial \nu_i}\left(\frac{F_i}{V k_B T}\right) + \lambda \frac{\partial}{\partial \nu_i}\Phi = 0.$$

Calculating the partial derivative,

$$\begin{aligned} 0 = \frac{\partial \mathcal{F}_i}{\partial \nu_i} &= \frac{\partial}{\partial \nu_i}\left(\nu_i\left[\ln(\nu_i \Lambda_i^3) - 1\right] - \nu_i(i-1)\frac{\epsilon}{k_B T} + \lambda b_1 i \nu_i\right) \\ &= \ln(\nu_i \Lambda_i^3) - (i-1)\frac{\epsilon}{k_B T} + \lambda b_1 i. \end{aligned}$$

Then at equilibrium the number of aggregates of length i per unit volume is

$$\nu_i = \Lambda_i^{-3} \exp\left[-\frac{\epsilon}{k_B T}\right] \exp\left[i\left(\frac{\epsilon}{k_B T} - \lambda b_1\right)\right]. \tag{2.8}$$

We wish to find λ so that we may calculate ν_i. Equations (2.8), (2.2), and (2.6) give

$$\frac{\Phi\, e^{\epsilon/k_B T}}{b_1 \left(\frac{2\pi\rho b_1 k_B}{h^2}\right)^{3/2} T^{3/2}} = \sum_{i=1}^{\infty} i^{5/2} e^{i\left(\frac{\epsilon}{k_B T} - \lambda b_1\right)}$$

which is graphed in Fig. 2.1 in the form

$$y = \sum_{i=1}^{\infty} i^{5/2} x^i \tag{2.9}$$

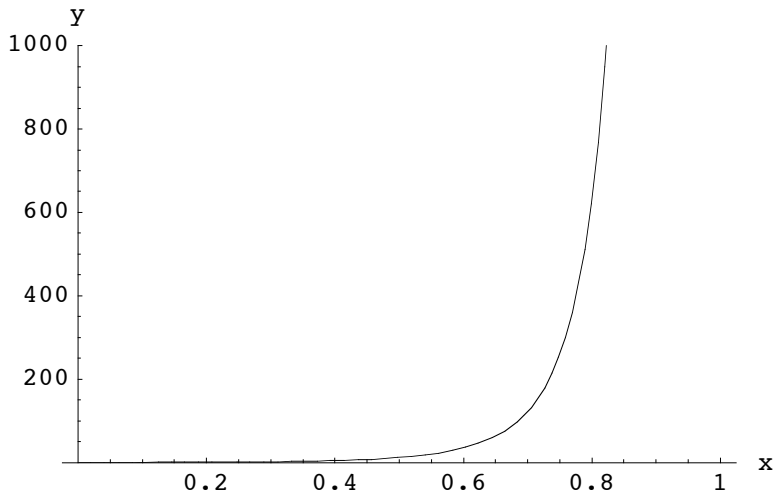

Figure 2.1: Equation (2.9) is used to find x for a given y and hence the Lagrange multiplier λ.

where

$$y \equiv \frac{\Phi\, e^{\epsilon/k_B T}}{b_1 \left(\frac{2\pi\rho b_1 k_B}{h^2}\right)^{3/2} T^{3/2}} \qquad \text{and} \qquad x \equiv e^{\left(\frac{\epsilon}{k_B T} - \lambda b_1\right)}. \tag{2.10}$$

Given y, it is possible to find x numerically using Mathematica's `FindRoot` function, as demonstrated in Appendix A. Then λ is given by Eq. (2.10) in the form $\lambda = \epsilon/b_1 k_B T - \ln x\,/b_1$.

Thus we can numerically calculate $\langle n \rangle$ for any given temperature and concentration, as follows. Experimentally, I have found that at a molar concentration of $c_m = 1.00$ M and a temperature of 49.9°C, Sunset Yellow FCF undergoes a phase transition between the isotropic phase and the isotropic-nematic coexistence phase (see Fig. 5.1 for experimental results). Using the equations of this section, we can calculate $\langle n \rangle$ for this concentration and temperature. First it is necessary to calculate the volume fraction of this sample.

In general, the concentration and the volume fraction of a solution are related. The volume fraction is

$$\begin{aligned} \Phi &\equiv \frac{V_{\text{solute}}}{V_{\text{solvent}} + V_{\text{solute}}} \\ &= \frac{m_{\text{solute}}/V_{\text{solvent}}}{m_{\text{solute}}/V_{\text{solvent}} + m_{\text{solute}}/V_{\text{solute}}} \end{aligned}$$

where m_{solute} is the mass of the solute (in this case, Sunset Yellow), m_{solvent} is the mass of the solvent (in this case, water), and V_{solute} and V_{solvent} are the respective volumes. Noting that the number of kilograms of dye per liter of water is $m_{\text{solute}}/V_{\text{solvent}} = M_w c$, where c is the concentration of the dye converted to units of mol/m^3 (i.e., $c = 1000$ L/m$^3 \times c_m$), and the

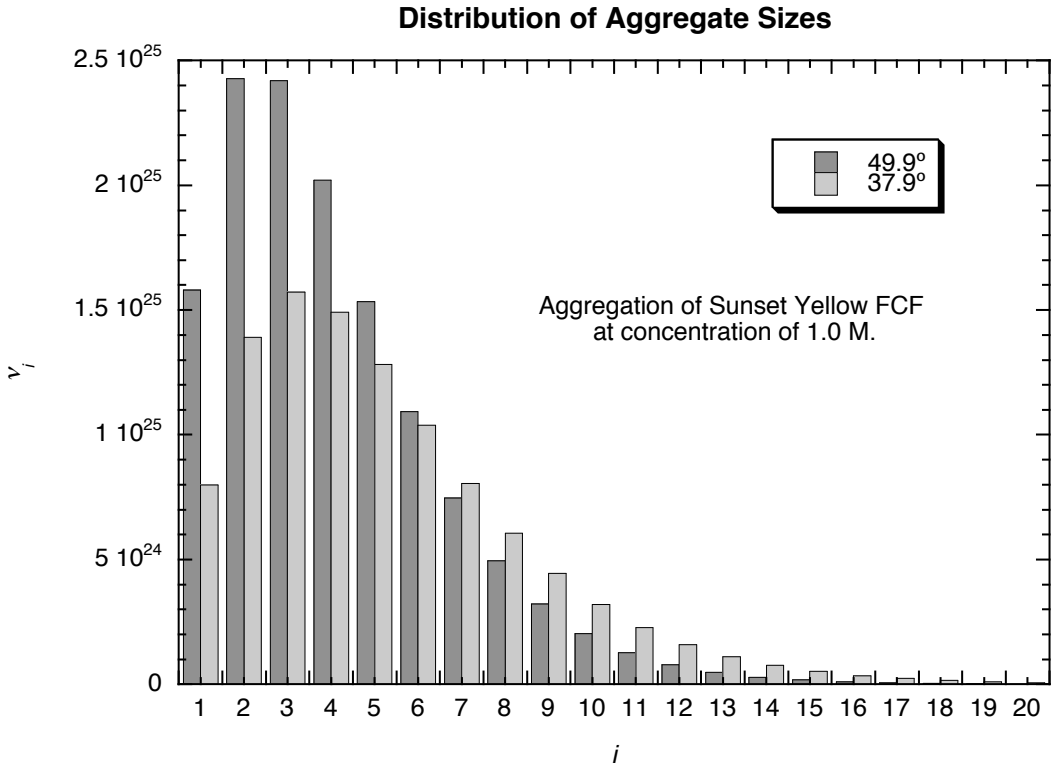

Figure 2.2: The number density ν_i of aggregates of length i, at a molar concentration of $c_m = 1.00$ M. At this concentration, the average number of molecules in an aggregate is $\langle n \rangle = 4.1$ at a temperature of $T = 49.9°$C and $\langle n \rangle = 5.2$ at $T = 37.9°$C. These two points on the phase diagram were chosen because they lie on the isotropic-coexistence curve and the coexistence-nematic curve, respectively (see the phase diagram results in Fig 5.1 on page 44).

density of the dye is $\rho = m_{\text{solute}}/V_{\text{solute}}$, we arrive at a convenient relation between volume fraction and concentration,

$$\Phi = \frac{M_w c}{M_w c + \rho}. \tag{2.11}$$

Note that ρ is much larger than $M_w c$, and so ρ dominates in the denominator. This shows that, although Eq. (2.11) is not a linear relation, the volume fraction is approximately proportional to the concentration.

Now we can calculate that a concentration of 1.00 M corresponds to a volume fraction of 0.244, so the phase change observed experimentally occurs at $\Phi = 0.244$ and $T = 323$ K. Using equations (2.11), (2.10), (2.9), (2.8), and (2.7), we find the distribution of aggregate lengths for this concentration and temperature, plotted in Fig. 2.2, and the average number of molecules in an aggregate, $\langle n \rangle = 4.1$ (see Appendix A).

2.1.2 Modeling the Phase Diagram

The method for calculating $\langle n \rangle$ allows us to predict the form of the phase diagram using only one experimental data point.

We will apply the Onsager approach, as described in Ref. [24]. This assumes that each aggregate is a hard rod with well-defined length L and diameter D. The only forces are due to collisions of the rods. The solution is assumed to be dilute, $\Phi \ll 1$, and the rods are long, $L \gg D$, so that end effects may be ignored.

These assumptions are likely too strong for a system with a distribution of aggregate lengths, where $L < D$ for many aggregates, including a significant number of monomers and dimers, and where Φ is around 0.24. However, the Onsager theory for nematics of hard rod solutions provides an interesting starting point for understanding the system and so we forge onwards.

According to the Onsager approach, the value of Φ for the isotropic phase in equilibrium with the nematic phase is

$$\Phi = 3.3\, D/L, \tag{2.12}$$

so, noting that the diameter D is constant, $\Phi L = 3.3\, D = \text{constant}$. Similarly, in the nematic phase, just at the transition point,

$$\Phi = 4.5\, D/L, \tag{2.13}$$

so $\Phi L = 4.5\, D = \text{constant}$. But the length of a rod is proportional to the number of molecules in the rod. On average this is $\langle n \rangle$, so

$$\Phi \langle n \rangle = \text{constant}$$

for points along the isotropic-coexistence curve or along the coexistence-nematic curve. We already have one point from that curve: for $c_m = 1.00$ M and $T = 49.9$°C, we have $\Phi \langle n \rangle = 1.0$. Using trial and error, for any concentration, we can find a temperature such that $\Phi \langle n \rangle = 1.0$, and this concentration and temperature is expected to fall on the isotropic-coexistence curve. Thus one experimental value, i.e. the temperature at which an 1.0-M solution crosses the isotropic-coexistence curve, yields the full curve theoretically.[3] The same is true of the coexistence-nematic curve, but first it is necessary to calculate a value on the coexistence-nematic curve. The diameter D of the rods is a constant independent of volume

[3]Given a value for D and for L, it is possible to predict a theoretical phase diagram from equations (2.12) and (2.13) with no experimental point. However, the theory breaks down at this point, and the resulting theoretical phase diagram is not found to be in close agreement with the experimental results.

fraction and temperature. For a given volume fraction, the length L of the rods in the solution is a function of temperature. By equations (2.12) and (2.13),

$$\frac{3.3}{L_{\text{iso-coex}}} = \frac{4.5}{L_{\text{coex-nem}}}$$

where $L_{\text{iso-coex}}$ is the length of a rod for a solution at the given volume fraction and on the transition point from an isotropic solution to a solution with coexistence, and $L_{\text{coex-nem}}$ is the length of a rod for a solution at the given volume fraction and on the transition point from a solution with coexistence to a nematic solution. Since the length of a rod is, on average, proportionate to the average number of molecules in an aggregate, we have

$$\frac{4.5}{3.3} = \frac{\langle n \rangle_{\text{coex-nem}}}{\langle n \rangle_{\text{iso-coex}}}. \tag{2.14}$$

Hence both the curves can be calculated given a single experimental data point. The result is shown in Fig. 2.3, and it suggests that the slope of the transition curves should be 56°C/M for the isotropic-coexistence curve and 50°C/M for the coexistence-nematic curve.

2.2 Anisotropy in Liquid Crystals

For a single particle of a liquid crystal, we can predict how a measured property of the liquid crystal phase is affected by the anisotropy of the molecule. This provides a way to empirically investigate the way the particles are ordered. This section will define the order parameter of a liquid crystal and derive an equation that will be used to find the order parameter of a liquid crystal with optical measurements.[4]

2.2.1 Anisotropy and Order Parameter

Suppose we choose a coordinate system based on a molecule, as shown in Fig. 2.4. Consider any tensor property

$$\mathbf{T} = \begin{pmatrix} T_{xx} & 0 & 0 \\ 0 & T_{yy} & 0 \\ 0 & 0 & T_{zz} \end{pmatrix} \tag{2.15}$$

where we have assumed that the tensor is diagonal because we are in the principle coordinate system of the molecule. Note that the trace is $\text{Tr}(\mathbf{T}) = T_{xx} + T_{yy} + T_{zz}$. We are interested in understanding what happens to this property $\mathbf{T}$ when it is measured in a different coordinate

[4]This section follows the argument in section 2.3 in Ref. [1].

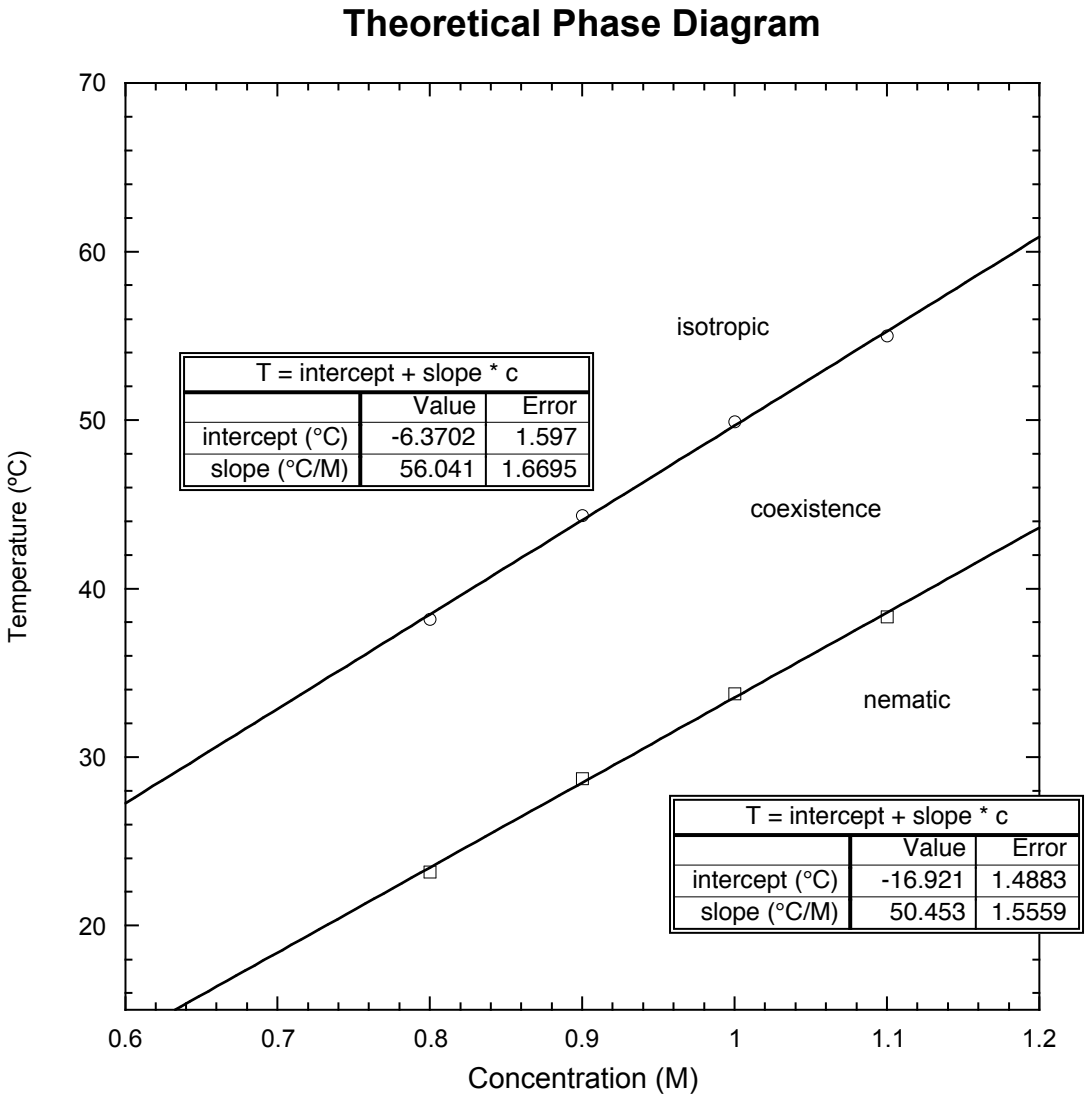

Figure 2.3: The theoretical phase diagram. We are able to calculate $\langle n \rangle$ for a given concentration and temperature. The Onsager result suggests that $\Phi\langle n \rangle$ is constant along the isotropic-coexistence curve and along the coexistence-nematic curve. On the isotropic-coexistence curve, the 1.0-M data point shown here is an experimental result, from Fig. 5.1. The 1.0-M data point on the coexistence-nematic curve is calculated by Eq. (2.14). The other points on each curve are calculated by holding $\Phi\langle n \rangle$ constant and varying the temperature and the concentration.

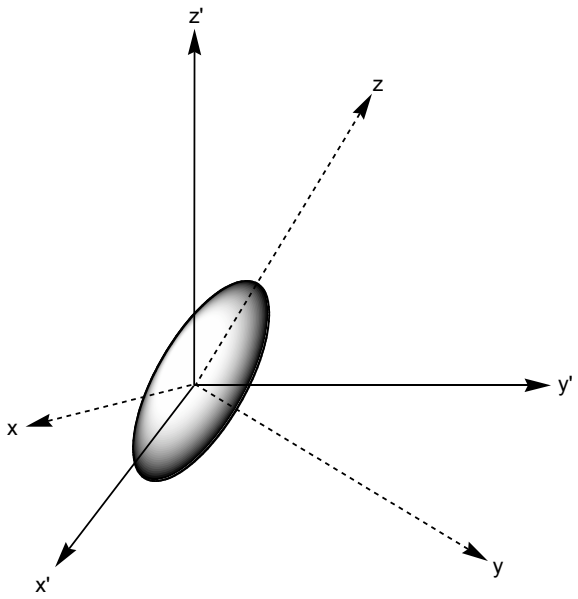

Figure 2.4: The coordinate system of a molecule. On the macroscopic level, it is convenient to use a coordinate system based on the director, the direction the molecules are pointing on average in in the liquid crystal sample. The director's coordinate system is shown here as the primed axes, with the z'-axis giving the direction of the director. However, each molecule may deviate from the director's coordinate system. We can speak of the molecule's own coordinate system, the unprimed system, and rotate between the two coordinate systems. It is assumed that the molecule has an axis distinct from the other axes. The z-axis follows the unique axis of this molecule. In the figure, the unique axis is shown as the long axis, but the unique axis of Sunset Yellow FCF is better described as the axis of the nitrogen-nitrogen double bond for some optical measurements. This is further discussed in section 6.1 on page 49.

system, namely, the coordinate system of the director. We will mathematically rotate twice by arbitrary angles φ about the z-axis and ϑ about the y-axis so that the direction is completely general. We call the rotated tensor property $\mathbf{T}'$.

$$\begin{aligned}
\mathbf{T}' &= R_y(\vartheta)\, R_z(\varphi)\, \mathbf{T}\, R_z^t(\varphi)\, R_y^t(\vartheta) \\
&= \begin{pmatrix} \cos\vartheta & 0 & -\sin\vartheta \\ 0 & 1 & 0 \\ \sin\vartheta & 0 & \cos\vartheta \end{pmatrix} \begin{pmatrix} \cos\varphi & \sin\varphi & 0 \\ -\sin\varphi & \cos\varphi & 0 \\ 0 & 0 & 1 \end{pmatrix} \begin{pmatrix} T_{xx} & 0 & 0 \\ 0 & T_{yy} & 0 \\ 0 & 0 & T_{zz} \end{pmatrix} \\
&\quad \times \begin{pmatrix} \cos\varphi & -\sin\varphi & 0 \\ \sin\varphi & \cos\varphi & 0 \\ 0 & 0 & 1 \end{pmatrix} \begin{pmatrix} \cos\vartheta & 0 & \sin\vartheta \\ 0 & 1 & 0 \\ -\sin\vartheta & 0 & \cos\vartheta \end{pmatrix}
\end{aligned}$$

This gives us a (somewhat complicated) matrix whose diagonal elements are

$$\begin{aligned}
T'_{x'x'} &= T_{xx}\cos^2\vartheta\cos^2\varphi + T_{zz}\sin^2\vartheta + T_{yy}\cos^2\vartheta\sin^2\varphi \\
T'_{y'y'} &= T_{yy}\cos^2\varphi + T_{xx}\sin^2\varphi \\
T'_{z'z'} &= T_{xx}\cos^2\varphi\sin^2\vartheta + T_{yy}\sin^2\vartheta\sin^2\varphi + T_{zz}\cos^2\vartheta.
\end{aligned}$$

Then, using some trigonometric identities, $\mathrm{Tr}(\mathbf{T}') = T_{xx} + T_{yy} + T_{zz} = \mathrm{Tr}(\mathbf{T})$. Hence the trace of the tensor property is invariant under rotation of the coordinate system.[5]

The anisotropy $\Delta T'$ for a liquid crystal is defined as the difference in properties between one axis (parallel to the director) and the average of the property along the other two axes (perpendicular to the director).

$$\begin{aligned}
\Delta T' &\equiv T'_{z'z'} - \frac{1}{2}(T'_{x'x'} + T'_{y'y'}) \qquad (2.16) \\
&= \frac{3}{2}T'_{z'z'} - \frac{1}{2}\mathrm{Tr}(\mathbf{T}') \qquad \text{[by the definition of trace]} \\
&= \frac{3}{2}T'_{z'z'} - \frac{1}{2}\,\mathrm{Tr}(\mathbf{T}) \qquad \text{[by the invariance of trace]} \\
&= \left(\frac{3}{2}\sin^2\vartheta\,\cos^2\varphi - \frac{1}{2}\right)T_{xx} + \left(\frac{3}{2}\sin^2\vartheta\,\sin^2\varphi - \frac{1}{2}\right)T_{yy} + \left(\frac{3}{2}\cos^2\vartheta - \frac{1}{2}\right)T_{zz}.
\end{aligned}$$

[5]In fact, rotation is a similarity transformation, a transformation that preserves angles and changes all distances in the same ratio (in the case of rotation, the ratio is 1), and therefore rotation preserves trace in general.

We follow convention in defining two order parameters,

$$\boxed{S \equiv \left\langle \frac{3}{2}\cos^2\vartheta - \frac{1}{2} \right\rangle \equiv \langle \mathrm{P}_2(\cos\vartheta)\rangle} \tag{2.17}$$

$$D \equiv \left\langle \frac{3}{2}\sin^2\vartheta\,\sin^2\varphi - \frac{1}{2} \right\rangle - \left\langle \frac{3}{2}\sin^2\vartheta\,\cos^2\varphi - \frac{1}{2} \right\rangle$$

where we take the average over values that are changing in time and changing from molecule to molecule and $P_2(x)$ is the second Legendre polynomial. Then the anisotropy is

$$\begin{aligned} \langle \Delta T' \rangle &= \left(-\frac{1}{2}S - \frac{1}{2}D\right) T_{xx} + \left(-\frac{1}{2}S + \frac{1}{2}D\right) T_{yy} + S\,T_{zz} \\ &= \left[T_{zz} - \frac{1}{2}(T_{xx} + T_{yy})\right] S + \frac{1}{2}\,(T_{yy} - T_{xx})\,D. \end{aligned} \tag{2.18}$$

We assume that the molecule is almost uniaxial such that $T_{zz} \neq T_{yy} \approx T_{xx}$. Then $T_{yy} - T_{xx}$ is small, so the first term in Eq. (2.18) dominates, and we will generally use S as the order parameter, not D.

2.2.2 A Formula for Measuring the Order Parameter

It is not obvious how to measure the order parameter S from its definition, Eq. (2.17). We will find that Eq. (2.18) leads to an equation for S such that S can be measured optically. We need to choose a material property of the liquid crystal as our tensor $\mathbf{T}$. The electric susceptibility $\boldsymbol{\chi}$ is a material property, but it isn't immediately obvious how to measure it.

What is the relationship between electric susceptibility and the absorption of the liquid crystal?

Consider an electromagnetic plane wave propagating in the $\hat{z}$ direction with wave number k, frequency ω, and complex amplitude $U = U_0\,e^{ikz}$. If the wave is propagating through some material, then it will cause a dipole moment per unit volume, or polarization $\vec{P}$, in the material. We assume that the material is a linear dielectric so that we may write $\vec{P} = \varepsilon_0 \boldsymbol{\chi} \vec{E}$, where $\varepsilon_0 = 8.85 \times 10^{-12}$ C^2/Nm^2 is the permittivity of free space. The constant of proportionality $\boldsymbol{\chi}$ is called the electric susceptibility tensor of the medium; we use a tensor rather than a scalar to account for the fact that it is generally easier to polarize a liquid crystal in some directions than in others. The permittivity of this material is defined as the tensor

$$\boldsymbol{\varepsilon} \equiv \varepsilon_0(\mathbf{1} + \boldsymbol{\chi}) \tag{2.19}$$

where $\mathbf{1}$ is the identity tensor [1, p. 195]. Let c be the speed of an electromagnetic wave in a

vacuum and let $v \equiv \omega/k$ be the speed of the electromagnetic wave in the material. Then the speed of light is $c = (\varepsilon_0\mu_0)^{-1/2}$, and analogously, $v = (\varepsilon\mu_0)^{-1/2}$, where $\mu_0 \equiv 4\pi \times 10^{-7}$ N/A^2 is the permeability of free space and ε is the component of the dielectric constant tensor for this direction [25]. Combining this with Eq. (2.19), we have

$$k = \frac{\omega}{c}\sqrt{1+\chi}. \tag{2.20}$$

Following Ref. [26], we consider the electric susceptibility to be complex, $\chi = \chi_r + \chi_{im}i$. Then the wavenumber k is also complex, showing that both the magnitude and the phase of the electric field vary with z. We split the complex wavenumber into its real and imaginary parts, writing for convenience

$$k = b + \frac{1}{2}ai$$

where a and b are real. Now $e^{ikz} = e^{ibz}e^{-\frac{1}{2}az}$, so that the intensity of the wave is attenuated by a factor $|e^{ikz}|^2 = e^{-az}$. For every distance of $1/a$ that the wave travels through the material, the intensity drops by a factor of e. Absorption A is the logarithm of the factor by which intensity is lowered,

$$A \equiv \log_{10}\frac{I(0)}{I(z)} = -\log_{10} e^{-az} = \frac{az}{\ln 10},$$

so for a given thickness z of material, $A \propto a$.

Assuming that $\chi_r \ll 1$ and $\chi_{im} \ll 1$, we can use a Taylor approximation of the square root in Eq. (2.20),

$$\begin{aligned} b + \frac{1}{2}ai = k &= \frac{\omega}{c}\sqrt{1+\chi_r+\chi_{im}i} \\ &= \frac{\omega}{c}\left(1 + \frac{\chi_r + \chi_{im}i}{2}\right). \end{aligned}$$

Equating the imaginary parts, we have $a = \frac{\omega}{c}\chi_{im} \propto \frac{v}{c}\chi_{im} = \chi_{im}/n$. Hence

$$\chi_{im} \propto nA. \tag{2.21}$$

Note that A depends on the orientation of light to the liquid crystal and n depends on the polarization of the light relative to the director of the liquid crystal. Since the electric susceptibility $\boldsymbol{\chi}$ is a material property of the liquid crystal, $\boldsymbol{n}A$ is also a material property, and we can use this to measure the order parameter S. In the discussion that follows, $\boldsymbol{\chi}$ is the imaginary part of the electric susceptibility tensor.

We assume that due to bonds on the molecule, only the z-component of the incident light is partially absorbed.[6] Then

$$\chi_{yy} = \chi_{xx} = 0, \tag{2.22}$$

and Eq. (2.18) becomes

$$\langle \Delta T' \rangle = \chi_{zz} S.$$

Combining this with Eq. (2.16) gives

$$\langle \Delta T' \rangle = \chi_{zz} S = \chi'_{z'z'} - \frac{1}{2}(\chi'_{x'x'} + \chi'_{y'y'}). \tag{2.23}$$

By Eq. (2.22) and the invariance of trace,

$$\mathrm{Tr}(\boldsymbol{\chi}') = \mathrm{Tr}(\boldsymbol{\chi}) = \chi_{zz}. \tag{2.24}$$

On the macroscopic level, the director is the only axis different from the others, so

$$\chi'_{y'y'} = \chi'_{x'x'}. \tag{2.25}$$

Applying this to Eq. (2.23) yields

$$\chi'_{z'z'} - \chi'_{x'x'} = \chi_{zz} S, \tag{2.26}$$

and applying Eq. (2.25) to Eq. (2.24), the trace of the tensor is

$$\chi'_{z'z'} + 2\chi'_{x'x'} = \chi_{zz}. \tag{2.27}$$

Dividing Eq. (2.26) by Eq. (2.27) gives

$$S = \frac{\chi'_{z'z'} - \chi'_{x'x'}}{\chi'_{z'z'} + 2\chi'_{x'x'}},$$

an equation for the order parameter that depends only on the imaginary part of the susceptibility in the primed (macroscopic) coordinate system. Writing this in terms of the absorption and the index of refraction, we have by Eq. (2.21)

$$S = \frac{n_{z'z'}A_{z'z'} - n_{x'x'}A_{x'x'}}{n_{z'z'}A_{z'z'} + 2n_{x'x'}A_{x'x'}}.$$

[6] In other words, when we apply Fig. 2.4 to the Sunset Yellow FCF molecule, we will choose the most absorbing bond as defining the molecule's z-axis. See Fig. 6.1 for more details about this bond.

At this point, the notation can be cleaned up a bit. The z' axis is the axis parallel to the director, and the x' axis is any axis perpendicular to the director. Thus we have

$$\boxed{S = \frac{n_\parallel A_\parallel - n_\perp A_\perp}{n_\parallel A_\parallel + 2n_\perp A_\perp}} \tag{2.28}$$

which gives the order parameter S in terms of optically measurable quantities.

2.2.3 The Order Parameter for an Aggregated System

The above argument is generally true of liquid crystals. In an LCLC, however, the particle making up the liquid crystal is an aggregate rather than a single molecule. The order parameter S given in Eq. (2.28) is the order parameter of the molecules, S_{molec}, not of the aggregate.

We will now consider the coordinate system of the aggregate, as shown in Fig. 2.5. As in Fig. 2.4, the z axis gives the unique direction of the molecule. The z' axis is the macroscopic director, i.e., the director for the aggregate long axes on average; it represents the laboratory coordinate system. The z'' axis is the direction of the aggregate long axis. In spherical coordinates in the z'' coordinate system, let (θ_1, ϕ_1) give the direction of the z' axis and let (θ_2, ϕ_2) give the direction of the unique axis of the molecule. Let γ be the angle separating the z and z' axes.

Applying the addition theorem for spherical harmonics [27, p. 746], we have a relation for the angles of Fig. 2.5 in terms of Legendre functions:

$$P_n(\cos\gamma) = P_n(\cos\theta_1)P_n(\cos\theta_2) + 2\sum_{m=1}^{n} \frac{(n-m)!}{(n+m)!} P_n^m(\cos\theta_1)P_n^m(\cos\theta_2)\cos m(\phi_1 - \phi_2).$$

The azimuthal angle ϕ_2 that the molecule makes with the aggregate coordinate system is not correlated with the azimuthal angle ϕ_1 the aggregate long axis makes with the director. Hence

$$\langle \cos[m(\phi_1 - \phi_2)] \rangle = 0,$$

so that on average every term of the summation vanishes. We assume that θ_2 is constant, i.e. that all molecules in the aggregate make an angle θ_2 with the long axis of the aggregate. Then

$$\langle P_2(\cos\gamma) \rangle = \langle P_2(\cos\theta_1) \rangle P_2(\cos\theta_2).$$

By Eq. (2.17), $\langle P_2(\cos\gamma) \rangle$ is the order parameter S_{molec} of the molecules, while $\langle P_2(\cos\theta_1) \rangle$

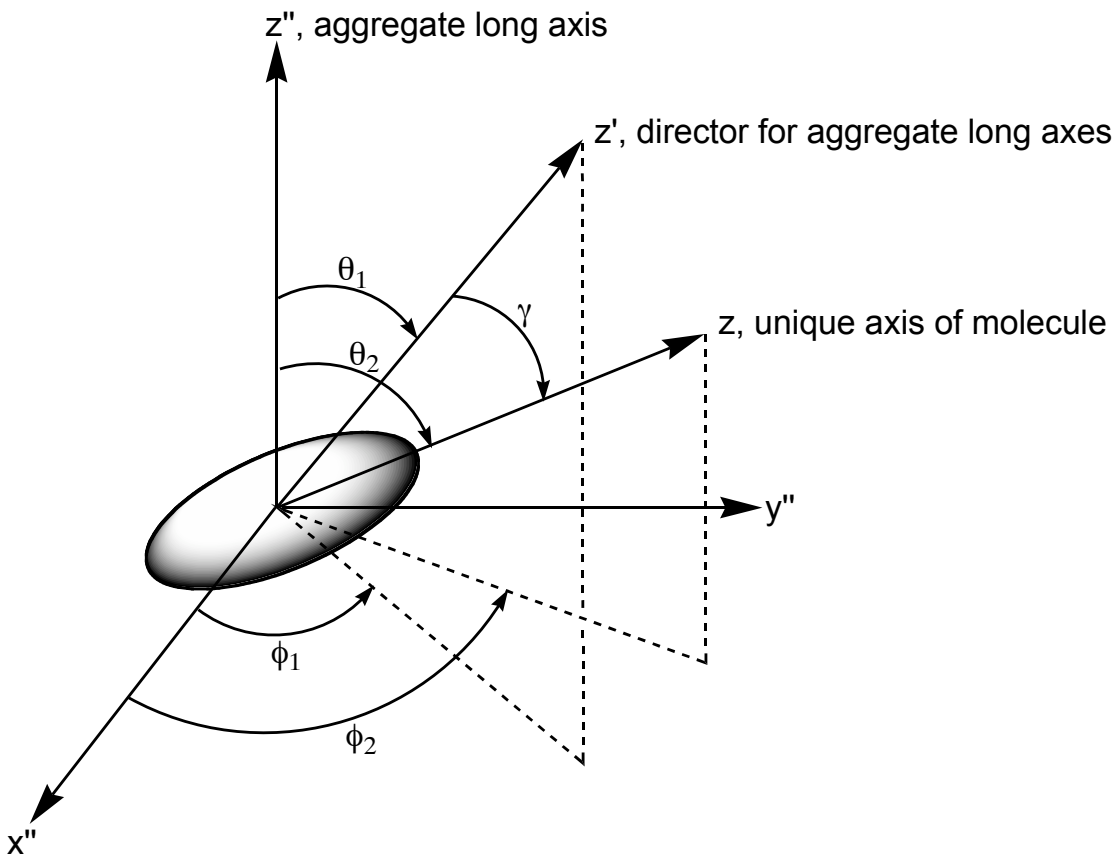

Figure 2.5: The coordinate system of an aggregate. The z and z' axes are the same ones shown in Fig. 2.4, with z giving the unique axis of a molecule in the aggregate and z' giving the direction of the director, the average direction of all aggregates. The z'' axis gives the direction of the long axis of the aggregate containing the molecule.

is the order parameter S_{agg} of the aggregate. Hence

$$\boxed{S_{\text{molec}} = S_{\text{agg}}\, P_2(\cos\theta_2).} \tag{2.29}$$

In section 6.1, this relation is used to calculate S_{agg} from the measurements of S_{molec}.

Chapter 3

Materials

3.1 Sunset Yellow FCF

Sunset Yellow FCF is an aggregated dye liquid crystal. It is a synthetic coal tar and azo yellow dye used as a food coloring (FD&C Yellow Number 6, or E110 in Europe). Its chemical name is the disodium salt of 6-hydroxy-5-[(4-sulfophenyl)azo]-2-naphthalenesulfonic acid, and its molecular structure is shown in Fig. 3.1. Pure Sunset Yellow FCF is a red-orange powder or crystal that is water-soluble. The Na and the OH groups of the molecule are hydrophilic, whereas the nonpolar aromatic rings tend to be slightly hydrophobic, and this promotes aggregation of the molecules to protect the aromatic rings from water. Interactions between the aromatic rings promote planar stacking, which also drives the tendency to aggregate.

The absorption spectrum for a dilute aqueous solution of Sunset Yellow FCF is shown in Fig. 3.2. Previous measurements show that the absorption spectrum of aqueous Sunset Yellow shifts as the concentration changes, indicating that aggregation of some sort occurs at every concentration of aqueous Sunset Yellow [22].

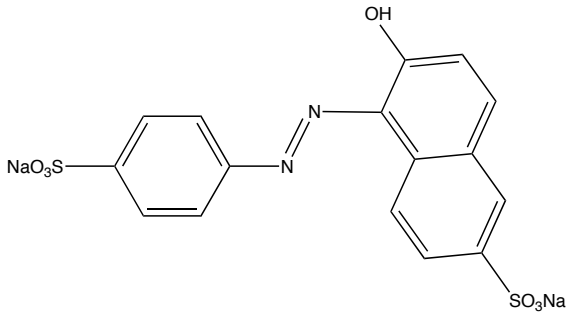

Figure 3.1: Sunset Yellow FCF is an azo yellow dye with aromatic rings. The molecule is planar, with a molecular weight of 452.38 amu.

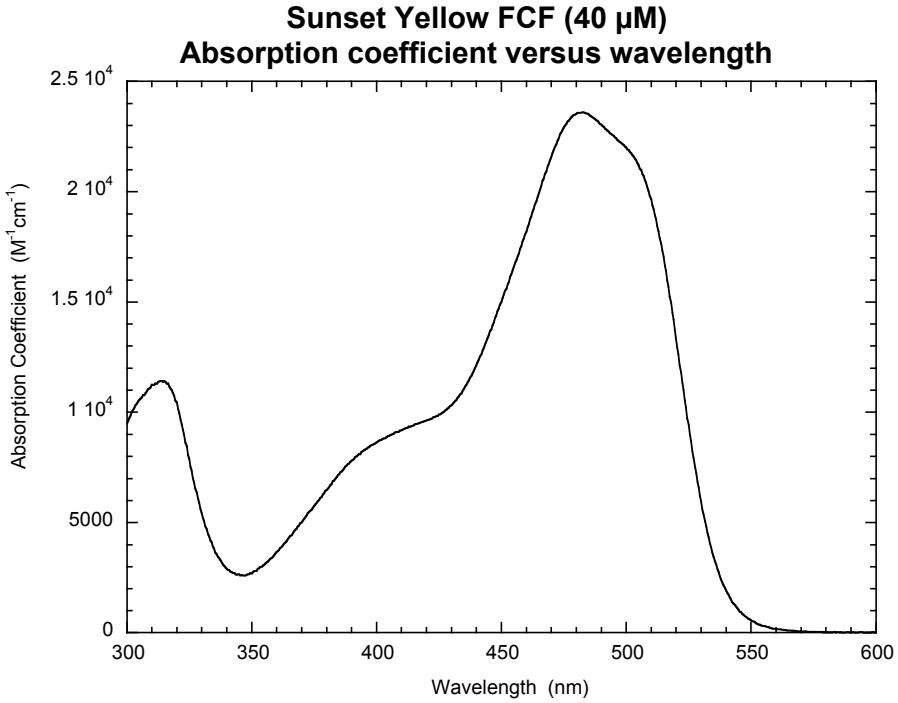

Figure 3.2: The absorption spectrum of isotropic aqueous Sunset Yellow FCF.

I prepared the aqueous solutions of Sunset Yellow in concentrations ranging from 0.8505 M to 1.102 M. The first difficulty in doing so was that solid Sunset Yellow absorbs moisture. In order to prevent this extra water from affecting the concentration of the solutions, I ground the solid Sunset Yellow with a mortar and pestle and put it under a vacuum overnight to dry. Afterwards, it was stored in the vacuum chamber.

I mixed aqueous solutions of Sunset Yellow by weighing a quantity of solid Sunset Yellow in a vial, then pipetting millipore water into the vial. I sealed the vial as soon as I had added the water. I mixed the dye with the water by placing the vial on a vortex mixer. Mixing a solution with the vortex mixer could take up to an hour for concentrations of 1 M and higher.

Chapter 4

Experimental Methods

4.1 Phase Diagram

The first step in taking measurements of Sunset Yellow FCF was to plot a phase diagram showing at what concentrations and temperatures the liquid crystal phase is stable.

In brief, the procedure for mapping the phase transitions was as follows: I first mixed the solution of dye, then sealed it in a glass cell. Sealing the cell was necessary to prevent evaporation that would alter the concentration of the solution. The cell was then placed on a heating stage under a microscope, between crossed polarizers, and slowly heated. As the dye heated, more and more of it changed from nematic to isotropic. I then cooled the sample and the sample changed from isotropic to nematic. The details follow.

I mixed each concentration of Sunset Yellow on the same day I used it for phase diagram measurements, so that the solution would not have much time to evaporate. Solutions were stored in sealed vials.

I used glass microscope slides, Devcon high strength two-part, two-ton all purpose epoxy adhesive, and 10-μm diameter glass fibers to make homemade glass cells, shown in Fig. 4.1. I mixed the epoxy with a small amount of glass fibers. I put a tiny drop of the mixture of epoxy and glass fibers on each of the four corners of a small rectangle of glass, then stuck this glass rectangle onto a larger rectangle of glass. I pressed the two pieces together, checking to see that they were parallel to each other by holding the cell under monochromatic light and ensuring that the interference fringes were not too close together. I wanted my cells to be sealed so that the water in the solutions would not evaporate. I tested a variety of glues, including silicon gel, KrazyGlue, Duco Cement, Devcon epoxy, PC-11 all-purpose white epoxy paste, and Weldbond Universal Space Age Adhesive to see which would best seal the glass cell. I found that both the Devcon epoxy and the PC-11 epoxy were reasonably good at sealing a cell, though both required time overnight to cure.

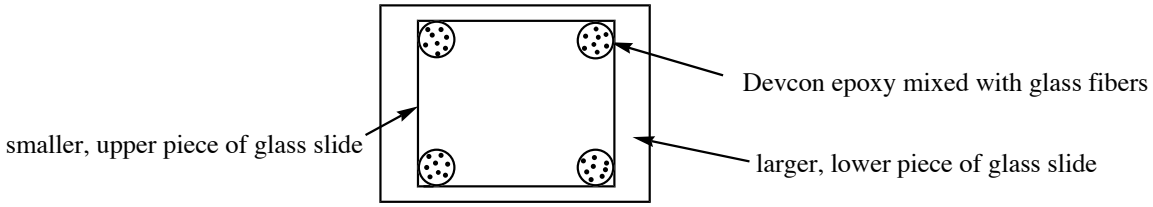

Figure 4.1: For the homemade cell, two pieces of a glass slide are glued together, spaced apart by 10-μm diameter glass fibers. With the glass pieces attached, two edges would be sealed with epoxy. This cell would then be filled with a sample of the dye and the remaining edges would be sealed with Critoseal (for the phase diagram measurements) or epoxy (for the birefringence and order parameter measurements) to prevent evaporation.

For each phase diagram cell, I sealed the edges of the cell together with Devcon epoxy. I left two gaps around the edge so that later there would be space to fill the cell with Sunset Yellow in solution. When I filled the cell, I would seal the gaps with Critoseal and immediately take measurements for the phase diagram. The Critoseal wasn't as effective as the epoxy at preventing evaporation, but it required no curing time, allowing measurements to immediately follow filling the cell.

I filled the cells by capillary action at room temperature. This could take several minutes as the capillary action slowly drew solution further into the cell. During this time, the solution was open to the air and would evaporate. To prevent this, I always filled the cells inside a humidity chamber, which was implemented as an oven with open plates of water. The humidity was generally between 90% and 100%, but it could fall to 60% if the door was open too long, so I left the cells inside the closed chamber while they were filling. Heating the oven while filling caused problems with the humidity and the water in the Sunset Yellow solutions would evaporate before the cell was filled, so I filled the cells at room temperature.

With the cells prepared, I was ready to take the phase diagram measurements. I taped each cell into a heating stage and placed it in a microscope between crossed polarizers, ramping the heating stage at 0.4°C per minute. I observed the phase changes while ramping up, noting the temperature where isotropic droplets first appeared and the temperature where the nematic droplets completely disappeared. Similarly, while ramping down I noted the temperature where the nematic droplets first appeared and the temperature where the isotropic droplets completely disappeared. The coexistence region was determined to be between the two temperatures for each ramping procedure. Figure 4.2 shows how the coexistence region looks under the microscope, between crossed polarizers. By following the above procedure, I was able to plot the phase diagram for the solution of Sunset Yellow in water. The phase diagram, once plotted, was an important tool when taking birefringence

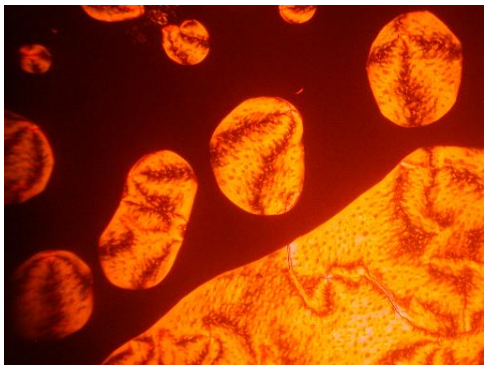

Figure 4.2: As the solution of Sunset Yellow passes between the isotropic phase and the nematic phase, patches of the solution are isotropic and patches are nematic. This is the coexistence, or two-phase, region. The colorful patches are nematic droplets while the darker areas are isotropic. This picture shows a cell that had evaporated until it was in the coexistence region at room temperature. The two phases occur simultaneously because the varying lengths of the aggregates cause the sample to behave like an impure solution. The droplets of liquid crystal shown here are about 0.5 mm wide.

measurements.

4.2 Birefringence

The first step was to determine how to analyze the data collected from the birefringence measurements. Birefringence is defined by $\Delta n \equiv n_e - n_o$, where n_e is the extraordinary index, which is only measured for one polarization direction of light, and n_o is the ordinary index, which is measured for a all polarizations of light that are perpendicular to the polarization for the extraordinary index. In this case, n_e is $n_\parallel$ and n_o is $n_\perp$, where $n_\parallel$ is the index of refraction for light polarized parallel to the director of the sample, and $n_\perp$ is the index of refraction for perpendicularly polarized light. Hence

$$\Delta n = n_\parallel - n_\perp. \tag{4.1}$$

Suppose λ_0 is the wavelength of the light outside the sample. Then the wavelength of the light while it passes through the cell depends on the polarization of the light:

$$\lambda_\parallel = \frac{\lambda_0}{n_\parallel} \quad \text{and} \quad \lambda_\perp = \frac{\lambda_0}{n_\perp}.$$

The retardation of the sample is $\delta \equiv \phi_{\parallel} - \phi_{\perp}$, where the phase angles $\phi_{\parallel}$ and $\phi_{\perp}$ are given by

$$\phi_{\parallel} = \frac{2\pi}{\lambda_{\parallel}} d \quad \text{and} \quad \phi_{\perp} = \frac{2\pi}{\lambda_{\perp}} d$$

where d is the thickness of the liquid crystal sample, so the birefringence is given by

$$\Delta n = \frac{\delta \lambda_0}{2\pi d},$$

or, in degrees,

$$\boxed{\Delta n = \frac{\delta \lambda_0}{360^\circ \, d}.} \tag{4.2}$$

By measuring the retardation angle δ of a sample of known thickness d, it is possible to arrive at the birefringence Δn of the sample. Furthermore, it is useful to note that we can treat the sample as a phase retarder for the purposes of calculating its effects on polarized light.

4.2.1 Jones Calculations

The Jones calculations here provide a way to calculate the polarization state of the light passing through the apparatus shown in Fig. 4.5.

I use a right-handed coordinate system where the x-axis is the horizontal, the y-axis is the vertical, and the z-axis is the direction of propagation of light. To calculate the amplitude of light passing through various optical components, I use Jones vectors and matrices, as described in Ref. [28].

A Jones vector represents the polarization state of light, with the x- and y-components of the vector each equal to the complex amplitude of the electric field in that direction. A Jones matrix represents an optical component that transforms the polarization state of light. In general, a retarder with the slow axis horizontal is represented by the Jones matrix

$$e^{i\delta/2} \begin{bmatrix} 1 & 0 \\ 0 & e^{-i\delta} \end{bmatrix},$$

and a retarder with the slow axis vertical is represented by the Jones matrix

$$e^{-i\delta/2} \begin{bmatrix} 1 & 0 \\ 0 & e^{i\delta} \end{bmatrix}$$

where δ is the retardation angle.

Suppose I rotate some optical element, such as a retarder, by an angle θ. This is equivalent to rotating the coordinate system by $-\theta$, so the components of this rotated optical element are equal to the unrotated optical element expressed in a frame rotated by $-\theta$. For example, a retarder with retardation δ oriented at some angle θ (where $\theta = 0^\circ$ represents a retarder with the slow axis horizontal) is represented by the matrix[1]

$$\begin{aligned} M_{\text{retarder}}(\theta) &= R(-\theta)\left(e^{i\delta/2}\begin{bmatrix} 1 & 0 \\ 0 & e^{-i\delta} \end{bmatrix}\right) R^t(-\theta) \\ &= \begin{bmatrix} \cos\theta & -\sin\theta \\ \sin\theta & \cos\theta \end{bmatrix} e^{i\delta/2} \begin{bmatrix} 1 & 0 \\ 0 & e^{-i\delta} \end{bmatrix} \begin{bmatrix} \cos\theta & \sin\theta \\ -\sin\theta & \cos\theta \end{bmatrix} \\ &= e^{i\delta/2}\begin{bmatrix} \cos^2\theta + e^{-i\delta}\sin^2\theta & \cos\theta\sin\theta - e^{-i\delta}\cos\theta\sin\theta \\ \cos\theta\sin\theta - e^{-i\delta}\cos\theta\sin\theta & \sin^2\theta + e^{-i\delta}\cos^2\theta \end{bmatrix}. \end{aligned}$$

The apparatus is set up such that horizontally polarized light passes through the liquid crystal, which is oriented with the director at $\theta = 45^\circ$ to the horizontal. The light then passes through a quarter wave plate with fast axis horizontal. I assume that the director of the liquid crystal is the slow axis, and use the matrix for a retarder oriented at $\theta = 45^\circ$,

$$\begin{aligned} M_{\text{LC}} &= e^{i\delta/2}\begin{bmatrix} \cos^2 45^\circ + e^{-i\delta}\sin^2 45^\circ & \cos 45^\circ\sin 45^\circ - e^{-i\delta}\cos 45^\circ\sin 45^\circ \\ \cos 45^\circ\sin 45^\circ - e^{-i\delta}\cos 45^\circ\sin 45^\circ & \sin^2 45^\circ + e^{-i\delta}\cos^2 45^\circ \end{bmatrix} \\ &= \frac{1}{2}e^{i\delta/2}\begin{bmatrix} 1+e^{-i\delta} & 1-e^{-i\delta} \\ 1-e^{-i\delta} & 1+e^{-i\delta} \end{bmatrix} \\ &= \begin{bmatrix} \cos\frac{\delta}{2} & i\sin\frac{\delta}{2} \\ i\sin\frac{\delta}{2} & \cos\frac{\delta}{2} \end{bmatrix}, \end{aligned}$$

to represent the liquid crystal. The quarter wave plate with fast axis horizontal and slow axis vertical is represented by the matrix

$$\begin{aligned} M_{\text{QWP}} &= e^{-i\beta/2}\begin{bmatrix} 1 & 0 \\ 0 & e^{i\beta} \end{bmatrix}, \qquad \text{where } \beta = \pi/2 \\ &= e^{-i\pi/4}\begin{bmatrix} 1 & 0 \\ 0 & i \end{bmatrix}. \end{aligned}$$

Then the state of the light that passes through the quarter wave plate is represented

[1]For background details on rotating matrices, see Appendix B.

by

$$\begin{aligned}
\text{QWP output} &= M_{\text{QWP}}\, M_{\text{LC}} \begin{bmatrix} 1 \\ 0 \end{bmatrix} \\
&= e^{-i\pi/4} \begin{bmatrix} 1 & 0 \\ 0 & i \end{bmatrix} \begin{bmatrix} \cos\frac{\delta}{2} & i\sin\frac{\delta}{2} \\ i\sin\frac{\delta}{2} & \cos\frac{\delta}{2} \end{bmatrix} \begin{bmatrix} 1 \\ 0 \end{bmatrix} \\
&= e^{-i\pi/4} \begin{bmatrix} \cos\frac{\delta}{2} \\ -\sin\frac{\delta}{2} \end{bmatrix}.
\end{aligned}$$

Only the mode of polarization is of interest here, so the amplitude of the light has been set equal to one.

The entire apparatus is rotated by some angle α, and then the light passes through a vertical polarizer with matrix $\begin{bmatrix} 0 & 0 \\ 0 & 1 \end{bmatrix}$. Mathematically,

$$\begin{aligned}
\text{final state} &= \begin{bmatrix} 0 & 0 \\ 0 & 1 \end{bmatrix} R(-\alpha) \left(e^{-i\pi/4} \begin{bmatrix} \cos\frac{\delta}{2} \\ -\sin\frac{\delta}{2} \end{bmatrix} \right) \\
&= \begin{bmatrix} 0 & 0 \\ 0 & 1 \end{bmatrix} \begin{bmatrix} \cos\alpha & -\sin\alpha \\ \sin\alpha & \cos\alpha \end{bmatrix} e^{-i\pi/4} \begin{bmatrix} \cos\frac{\delta}{2} \\ -\sin\frac{\delta}{2} \end{bmatrix} \\
&= e^{-i\pi/4} \begin{bmatrix} 0 \\ \sin\alpha\cos\frac{\delta}{2} - \cos\alpha\sin\frac{\delta}{2} \end{bmatrix}.
\end{aligned}$$

Note that the final state is $\vec{0}$ whenever α equals $\frac{\delta}{2} + p\pi$, where p is any integer.

Hence, when the light is extinguished, the angle α that the apparatus has been rotated is equal to $\frac{\delta}{2} + p\pi$. In conclusion, if I know the integer p, then rotating the apparatus so as to extinguish the light gives the retardation of the liquid crystal by the formula

$$\delta = 2(\alpha - p\pi),$$

or, in degrees,

$$\boxed{\delta = 2(\alpha - p\,180^\circ).} \tag{4.3}$$

Combining equations (4.2) and (4.3) gives an equation for analyzing the data and so I was able to begin taking measurements.

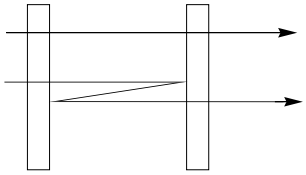

Figure 4.3: The path of light in an empty cell. Light may pass through the glass or it may be reflected some number of times. Constructive interference occurs when half-waves of light fit exactly between the top and bottom pieces of glass. Shown here are two possible paths, with the lower path one wavelength longer than the upper path. There are two 180° phase shifts such that the rays following the two paths are in phase with each other.

4.2.2 Procedure for Birefringence Measurements

I prepared glass cells as shown in Fig. 4.1, but before attaching the pieces of glass together with Devcon epoxy, I rubbed the both glass pieces firmly with felt in the same direction on the side of the glass that would be inside the cell, in order to promote alignment of the liquid crystal. Solutions of Sunset Yellow are more difficult to align than typical thermotropic liquid crystals. When I filled these cells with aqueous Sunset Yellow, the rubbing direction determined the director. There were occasional scratches, but it was possible to avoid them when taking measurements on the cell. The cells were sealed with PC-11 epoxy.

Prior to filling a glass cell with the liquid crystal sample, it was necessary to measure the thickness of the cell. I used an optical method, measuring the transmission peaks in a UV-Vis spectrophotometer. In the empty cell, we can assume that constructive interference occurs when half-waves of light fit exactly between the top and bottom pieces of glass as shown in Fig. 4.3, creating a trough on the absorption spectrum of the empty cell. If q_0 half-waves fit in the cell, where q_0 is an integer, then

$$q_0 \frac{\lambda_0}{2} = d \tag{4.4}$$

where d is the thickness of the cell and λ_0 is the wavelength of the light. Each absorption trough measured represented a different number of standing waves fitting in the glass cell, so each peak was assigned a number, starting at $q = 1$. I let q_0 be the number of half-waves that fit inside the cell for the trough just below in wavelength the one labeled $q = 1$. Then the data was fit to Eq. (4.4) in the form

$$\lambda_q = \frac{2d}{q_0 - q}, \tag{4.5}$$

giving d and q_0 as fitting constants, as shown in Fig. 4.4. Hence I optically measured the

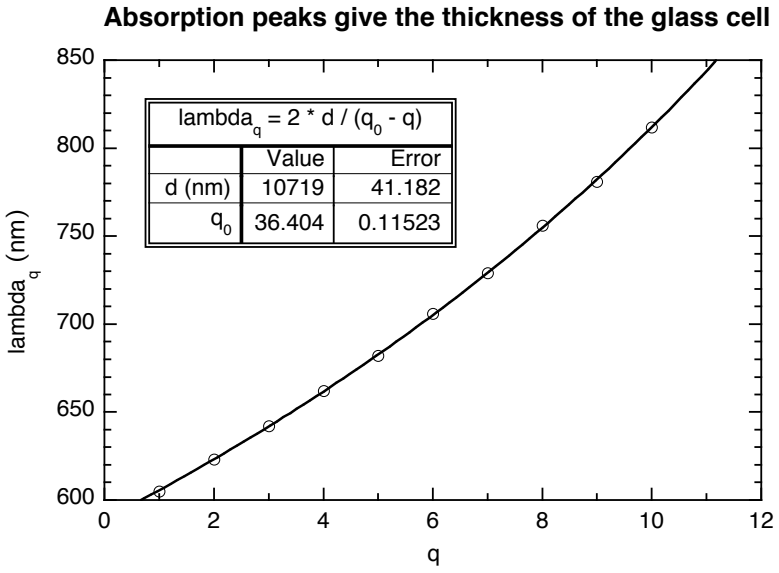

Figure 4.4: Each peak in the absorption spectrum represents the standing waves of the light fitting precisely within the cell, such that there must be an integer number of half-waves. The wavelength λ_q of each peak is shown in the figure. By using Eq. (4.5) to curve-fit the data, the optical thickness of this particular cell is $d = 10.72 \pm .04$ μm for this particular cell. This cell was then used for birefringence measurements (see Fig. 5.2 on page 45).

thickness of the glass cell.

Now I was ready for birefringence measurements. I filled a felt-rubbed glass cell with a solution of Sunset Yellow, and sealed the cell to slow the evaporation. I observed the cell under a microscope and chose a well-aligned region without disclinations or air bubbles for use in the birefringence measurement. I taped the cell of Sunset Yellow onto a heating stage so that this well-aligned region was visible.

For birefringence measurements, I used a binocular microscope with a light detector replacing one of the eyepieces. I used the other eyepiece to observe the sample during the measurement, and to identify the temperature at which it reached coexistence. The apparatus was set up as shown in Fig 4.5. For more details of the procedure, see Appendix C.

The retardation δ in degrees is given by Eq. (4.3), and the birefringence Δn is given by Eq. (4.2). But first, applying Eq. (4.3) requires one more piece of information: the value of p.

4.2.3 Resolving the Ambiguity in Birefringence Measurements

Equation (4.3) is ambiguous. The light is extinguished whenever α equals $\frac{\delta}{2} + p\pi$ for any integer p, where p represents the number of half-rotations of the sample. By picking a differ-

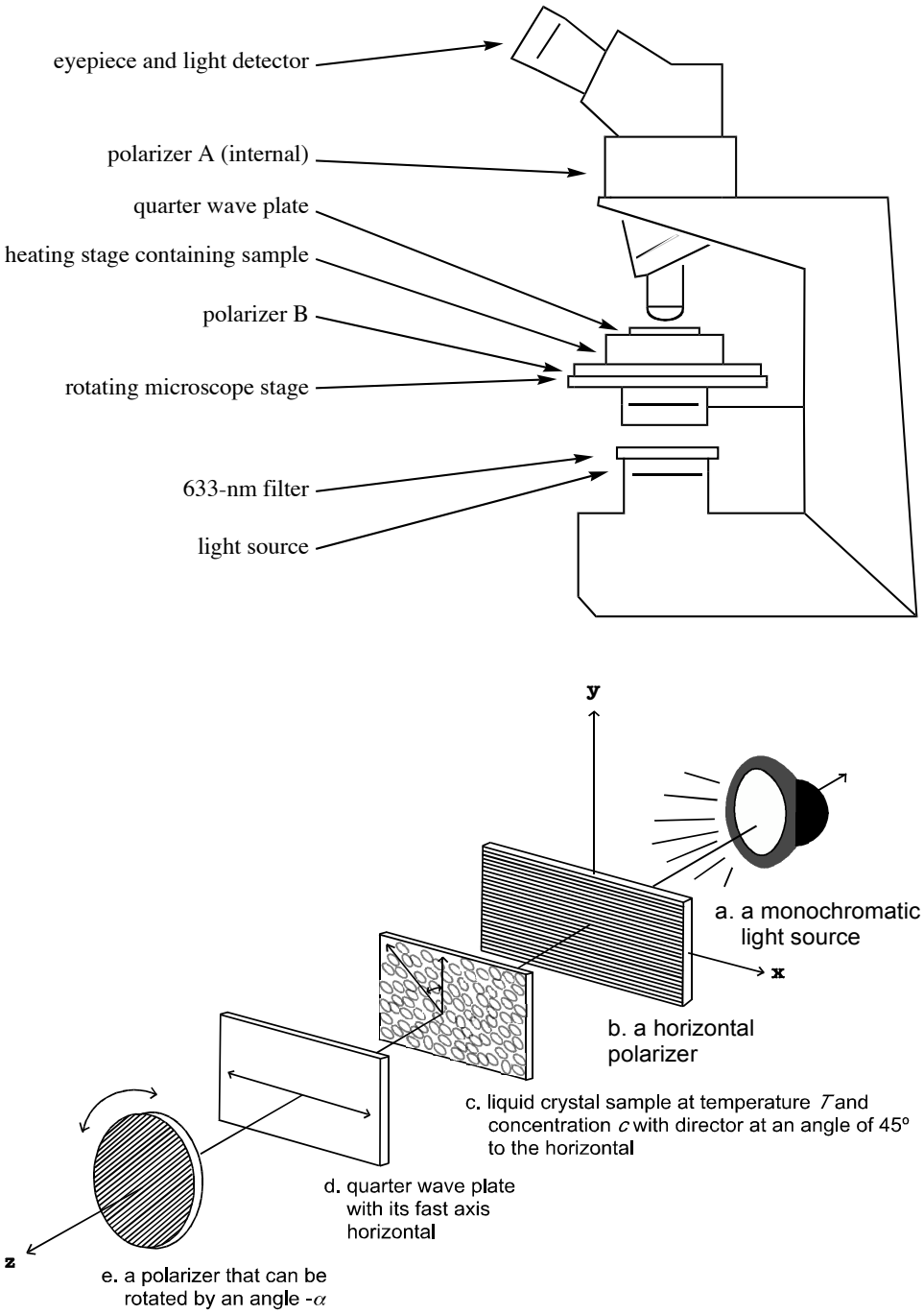

Figure 4.5: Two views of the apparatus for birefringence measurements on the binocular microscope. Light passes through a 633-nm filter, then polarizer B, the sample, and a quarter wave plate, which rotate together on the microscope stage. The light then passes through a 10x objective lens and polarizer A before it is detected by the light detector. One eyepiece is left in place for observation while the other has been removed with a light detector taped in its place.

ent value of p when analyzing the measurements of α, it is possible to shift all birefringence measurements in increments of $\frac{\lambda_0}{d}$.

To narrow down p, I used a glass cell of smaller thickness d. Decreasing d had the effect of increasing the increment size between possible values of Δn for a given α measurement. There was only one value for p for each sample that yielded a gradual decrease[2] in birefringence as the concentration was increased. This value of p was used for all measurements.

4.3 Order Parameter

I found the order parameter S using Eq. (2.28) by measuring the absorption by the liquid crystal of light polarized both parallel to and perpendicular to the director and by measuring the index of refraction for light polarized both parallel to and perpendicular to the director of the sample.

The procedure for measuring the absorption of the liquid crystal sample was as follows. I assembled a felt-rubbed glass cell of optical thickness $d = (10.415 \pm 64)$ μm, measured with the UV-Vis spectrophotometer with the method described in section 4.2.2, and filled it in the humidity chamber at 50°C with 0.9500-M Sunset Yellow FCF. The cell was sealed with PC-11 epoxy to avoid rapid evaporation. Measurements were taken two days after filling. During the order parameter measurements, the sample was heated to 77°C and never changed phase, suggesting that the sample was in fact much more concentrated than it had been when it was filled.

The apparatus is shown in Fig. 4.6. A light detector was placed over one ocular of a binocular microscope. The polarizers were initially crossed. The cell was taped into a heating stage, and the heating stage was placed under the microscope, between the crossed polarizers. The heating stage was rotated until the director of the liquid crystal, pointing in the direction the glass had been rubbed with felt, was parallel to the top polarizer. In this orientation, the light detector measured a minimum of light passing through. The lower polarizer was rotated by 90° so that the polarizers were now parallel.

With the 576-nm filter, the light measured was of low intensity, and it was necessary to minimize extraneous light sources by turning off all lights in the laboratory and covering the unused eyepiece. The detector had to be calibrated to ensure accuracy to within 1 nW.

The heating stage and liquid crystal sample were now rotated until the light was maximized. The angle and the power of the light detected were noted. The stage and

[2]That is, a gradual increase in the absolute value of the birefringence.

sample were then rotated by 90° and the power was noted. The sample was then heated and the power was noted at those same two angles.

The procedure was repeated for a cell filled with pure water to establish a base when no absorption is present, $A_{\text{water base}} = 0$. Then the absorption was calculated using[3]

$$A_\perp = \log_{10}\left(\frac{\text{intensity of base}_\perp}{\text{intensity of sample}_\perp}\right) \qquad \text{and} \qquad A_\parallel = \log_{10}\left(\frac{\text{intensity of base}_\parallel}{\text{intensity of sample}_\parallel}\right).$$

It remained to determine $n_\parallel$ and $n_\perp$. The first step was to measure n_{iso}, the index of refraction of isotropic aqueous Sunset Yellow FCF. I used an Abbe refractometer, a device that uses total internal reflection to determine the index of refraction of an isotropic liquid. In effect, I was using

$$\sin\theta_{\text{crit}} = \frac{n_1}{n_2}$$

where θ_{crit} is the critical angle, n_1 is n_{iso}, and n_2 is a known index of refraction for glass in the refractometer. The refractometer used a sodium lamp with light of wavelength $\lambda = 589$ nm, so it was necessary to correct this measurement to find n_{iso} for 633-nm light. By focusing the instrument, it was possible to measure $n_{486} - n_{656}$, the difference between the indices of refraction for light of wavelength 486 nm to that of light of wavelength 656 nm. From this measurement, I followed the instructions in the refractometer manual to interpolate n_{iso} for a light wavelength of 633 nm. This was measured at room temperature; I assumed temperature changes wouldn't change the value of n_{iso} substantially. Using a linear curve fit, I could calculate the isotropic index of refraction for any concentration relatively close to my measurements, including concentrations for which there exists no isotropic phase of Sunset Yellow FCF at room temperature. I chose a concentration of 1.25 M as a good estimate for the concentration of the sample whose absorption I had measured. At this point, there are clearly a number of approximations and corrections involved in finding n_{iso}. Changing the value of n_{iso} was found to have little effect on the value of S, so the approximations for n_{iso} were quite reasonable.

Thus I had 633-nm wavelength values for n_{iso} and Δn as it varied with temperature[4]. What does it mean to extrapolate n_{iso} to a concentration and temperature where the dye is in the liquid crystal phase, not isotropic? In the liquid crystal phase, there are two indices, $n_\perp$ and $n_\parallel$, not one, but we would expect that some sort of average of these two indices gives n_{iso}. It is necessary to take the average of a material property of the liquid crystal. The permittivity $\boldsymbol{\varepsilon}$ defined in Eq. (2.19) is a material property, and so taking the average

[3]Power was measured whereas intensity is required to calculate the absorption, but the area of the light detector remains constant, so the power measurements give the correct ratio.

[4]I used the measurements of Δn from the 1.25-M data in Fig. 5.2.

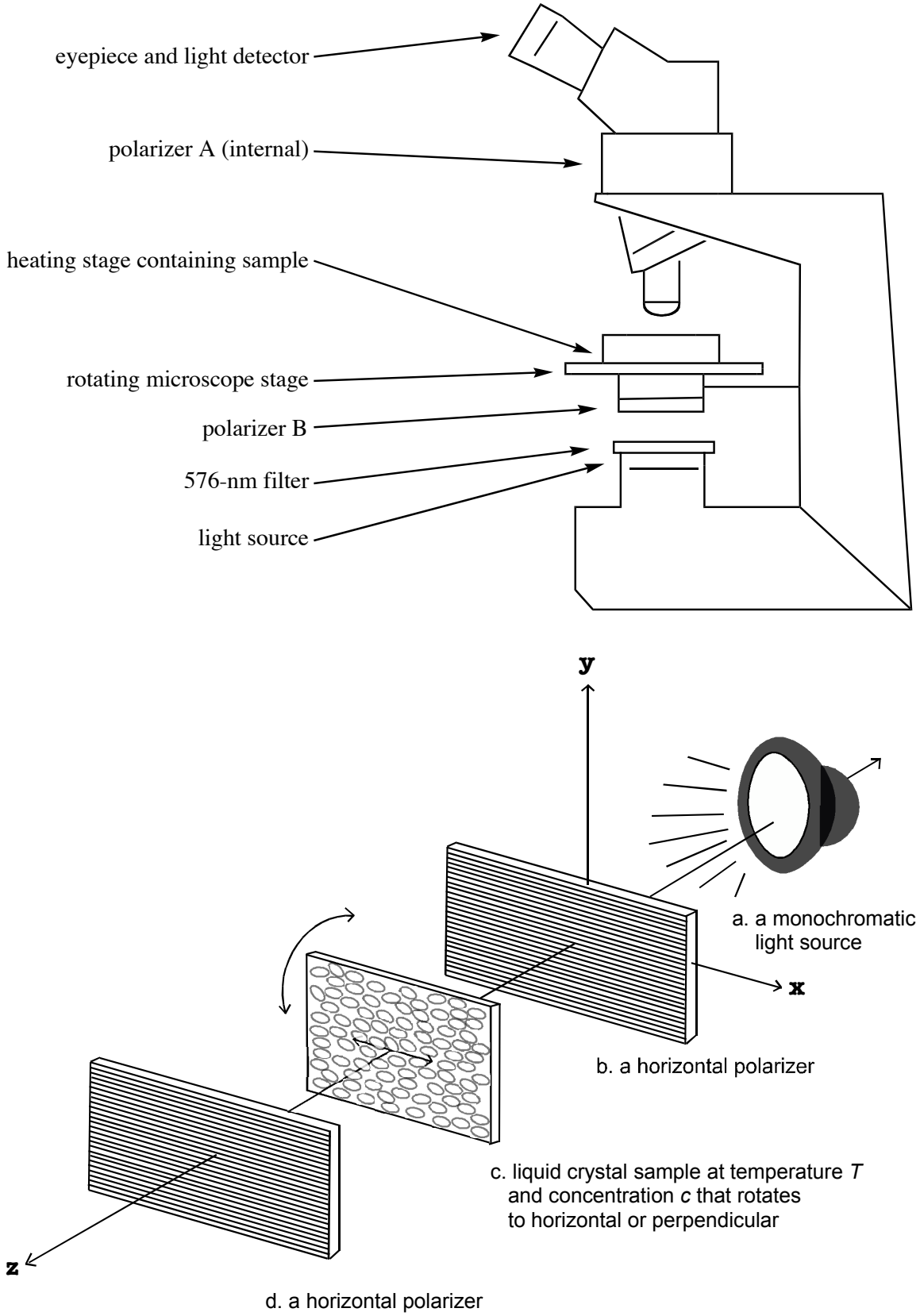

Figure 4.6: Two views of the apparatus for order parameter measurements.

has physical meaning. The average permittivity is

$$\varepsilon_{\text{avg}} = \frac{\varepsilon_{\parallel} + 2\varepsilon_{\perp}}{3} \tag{4.6}$$

where the average is taken over the three dimensions, with the two perpendicular directions assumed to be equal. It is straightforward to convert this to an equation for the more-easily measured index of refraction. Let c be the speed of light in vacuum and let v be the speed of light in the material. Recall that $c = (\varepsilon_0\mu_0)^{-1/2}$ and $v = (\varepsilon\mu_0)^{-1/2}$. But since $n \equiv \frac{c}{v}$, we have $n^2 = \frac{\varepsilon}{\varepsilon_0}$. Then Eq. (4.6) becomes

$$n_{\text{iso}}^2 = \frac{n_{\parallel}^2 + 2n_{\perp}^2}{3}.$$

Combining this with Eq. (4.1) and applying the quadratic formula[5] gives

$$\boxed{\begin{aligned} n_{\parallel} &= \tfrac{2}{3}\Delta n + \sqrt{-\tfrac{2}{9}\Delta n^2 + n_{\text{iso}}^2} \\ n_{\perp} &= -\tfrac{1}{3}\Delta n + \sqrt{-\tfrac{2}{9}\Delta n^2 + n_{\text{iso}}^2}, \end{aligned}} \tag{4.7}$$

providing a way to measure $n_{\parallel}$ and $n_{\perp}$, and so, by Eq. (2.28), I arrived at S as it varies with temperature.

[5]The positive square root is chosen because $n_{\parallel}$ and $n_{\perp}$ are expected to be close to positive n_{iso}.

Chapter 5

Experimental Results

5.1 Phase diagram

The Sunset Yellow FCF phase diagram shown in Fig. 5.1 illustrates how the phase of aqueous Sunset Yellow varies with temperature and concentration.

While the heating stage was ramping up or down, the sample of Sunset Yellow did not quite keep up with the temperature of the stage. Temperatures measured while heating were higher than temperatures measured while cooling. Each data point on the phase diagram actually represents two measured data points: the top of the error bar and the bottom of the error bar. The top of the error bar is the temperature of the heating stage when the solution changed phase while heating, whereas the bottom of the error bar is the temperature of the heating stage when the solution changed phase while cooling. I assumed that the average of these two points was a more accurate measurement of the phase transition temperature.

5.2 Birefringence

The results from the birefringence measurements are shown in Fig. 5.2. The ambiguity in Eq. (4.3) made it difficult to determine exactly what the birefringence was, since at first it wasn't clear which p to use in analyzing the data. However, this was resolved. First, as a substance is heated, the disorder will increase, so the anisotropy will decrease and hence I expect the absolute value of the birefringence to decrease. Since the curves in Fig. 5.2 all curve upwards, the birefringence must be negative. A material with negative birefringence is said to be negative uniaxial. Then, as described in section 4.2.3, I measured α for a thin cell, with an optical thickness of 4.7 μm. This placed Δn in the region of -0.07 to -0.11.

For the thinner cell, I used a commercial cell. The glass of the commercial cell had

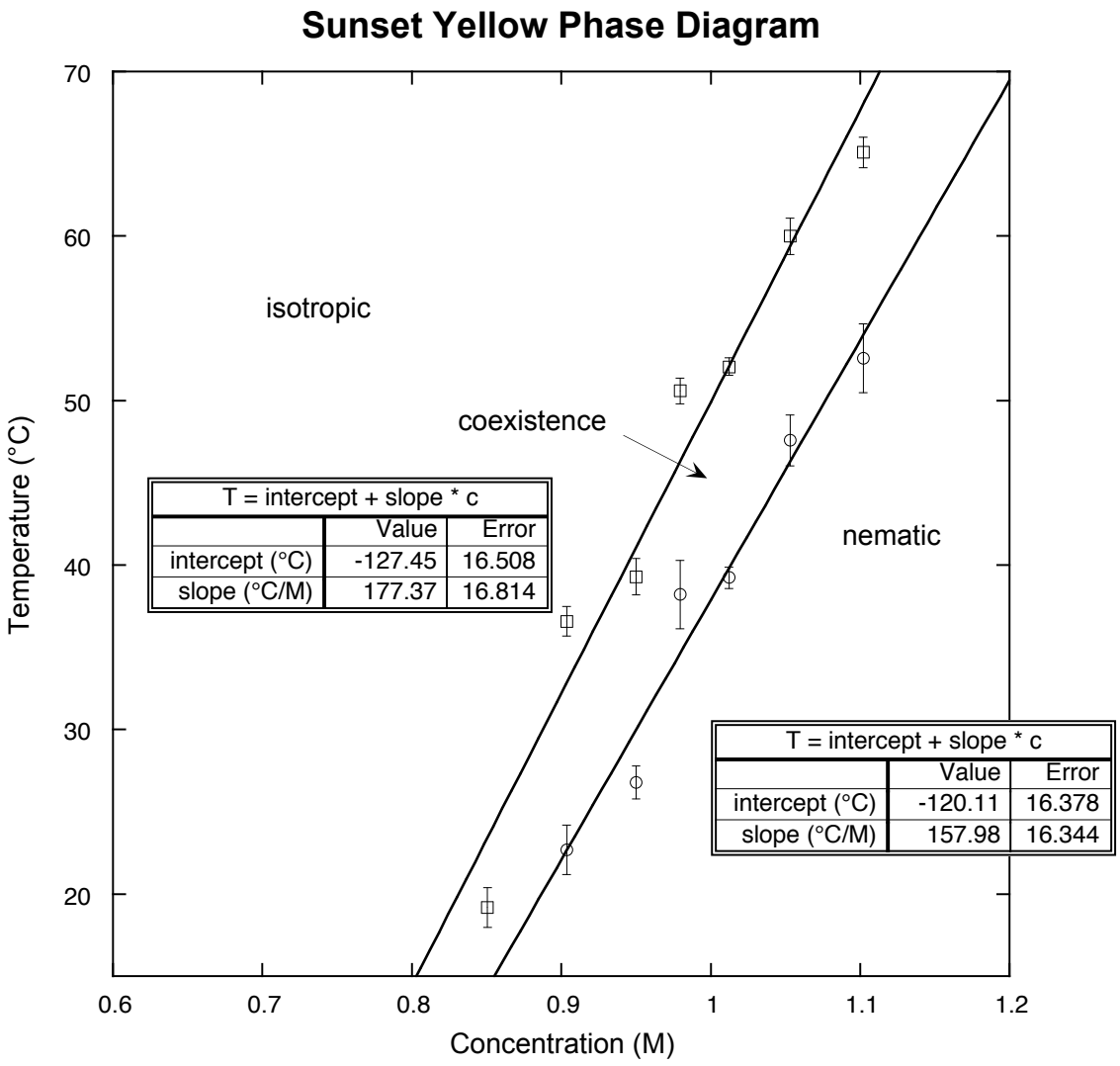

Figure 5.1: The phase diagram for Sunset Yellow FCF shows how the phase of the solution depends on the concentration and the temperature. The linear curve-fit is for convenience; it is not expected that the curve appears linear on larger scales.

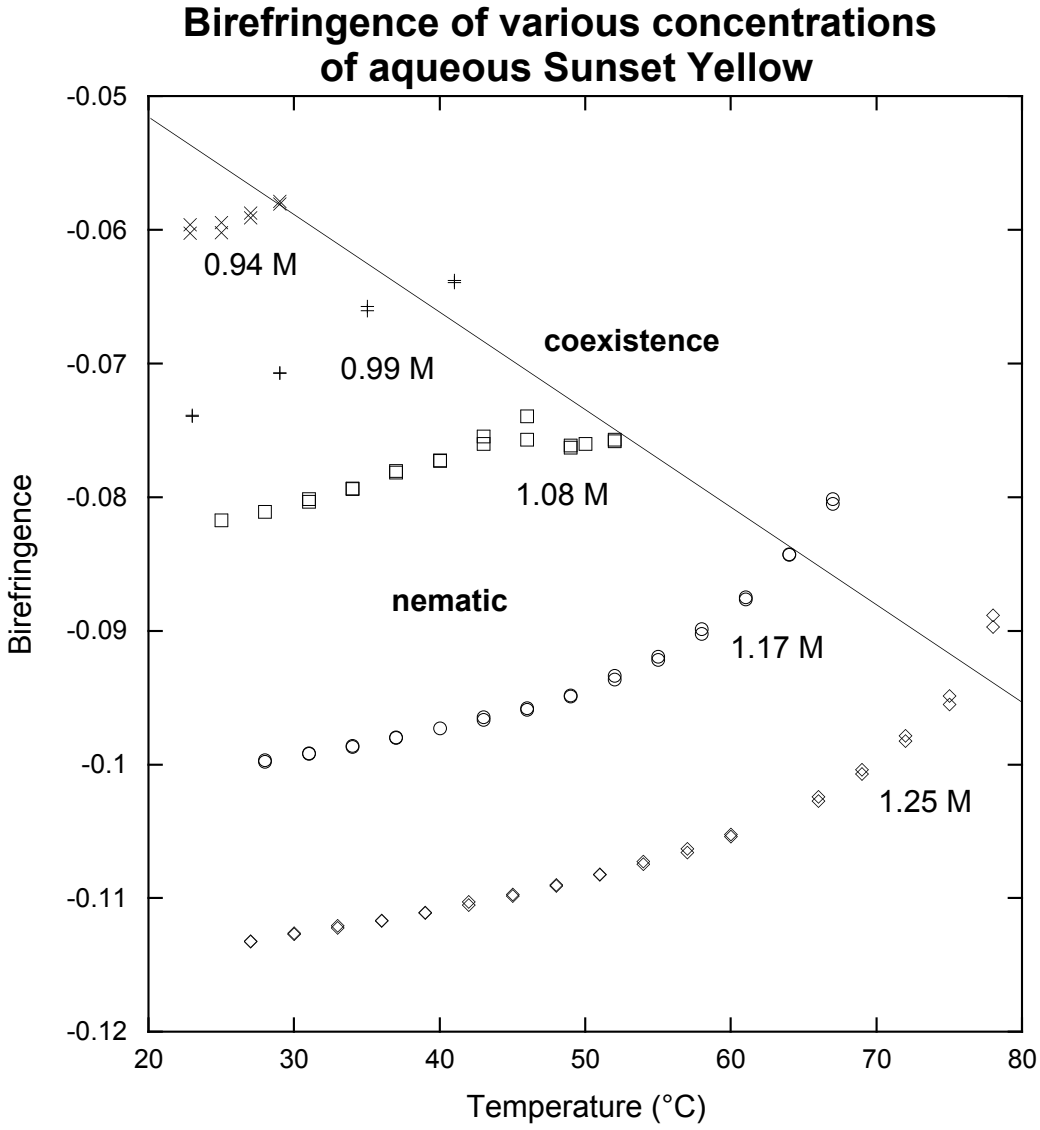

Figure 5.2: Each of the five birefringence curves shows how the birefringence of aqueous Sunset Yellow changes as it is heated. The data were taken for nematic samples, except the last data point on each curve, which was taken after the sample had reached coexistence. There appears to be a linear relation between the temperature at which a sample of a given concentration reaches coexistence (which gives the concentration) and the birefringence at that temperature, as shown by the line drawn on the figure. Two cells were used for these measurements: a 10.7-μm homemade felt-rubbed cell and a 4.7-μm commercial cell with (0.94-M solution). The concentrations shown are calculated from the phase transition temperature and Fig. 5.1.

been coated with a polymer and rubbed to promote alignment of the director. The dye solution didn't flow easily into the cell, so I used a vacuum to draw the solution into the cell, and used a concentration that was isotropic at room temperature. After sealing the cell, I waited ten days for water to slowly evaporate through the epoxy seal, so that the sample inside the cell became more concentrated, until it passed through the concentration where its phase changed to a liquid crystal.

I observed the hexagonal M phase with herringbone texture in samples that had become more concentrated through evaporation. No measurements were taken of these samples.

5.3 Order Parameter

The index of refraction of isotropic Sunset Yellow FCF is shown in Fig. 5.3 as a function of concentration. A linear curve fit of this plot is used to approximate n_{iso} at a concentration of 1.25 M. Once I correct for variation in index due to wavelength, $n_{\text{iso}} = 1.47 \pm 0.01$. Combining this value of n_{iso} with the birefringence Δn (for the 1.3-M sample in Fig. 5.2) as a function of temperature, Eq. (4.7) gave $n_{\parallel}$ and $n_{\perp}$. Then the absorption data and the index of refraction data yield the order parameter, shown in Fig. 5.4. This is the order parameter of the molecules S_{molec}, as noted in section 2.2.3. The order parameter of the aggregate S_{agg} is calculated in section 6.1.

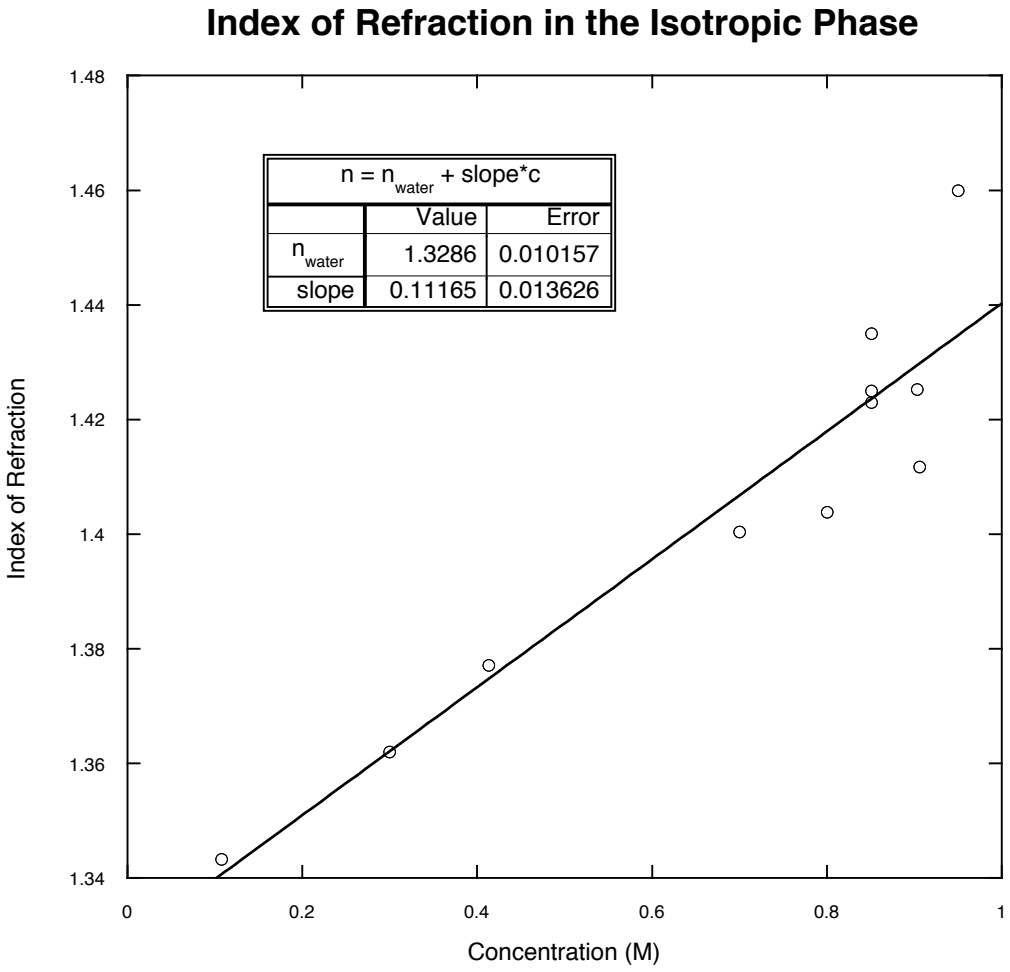

Figure 5.3: The index of refraction at room temperature, measured using a refractometer with a light wavelength of 589 nm. The concentrations of the solutions have a large error. These results give $n_{\text{iso}} = (1.33 \pm 0.01) + (0.11 \pm 0.01)c_m$ M^{-1}, where c_m is the molar concentration of the solution.

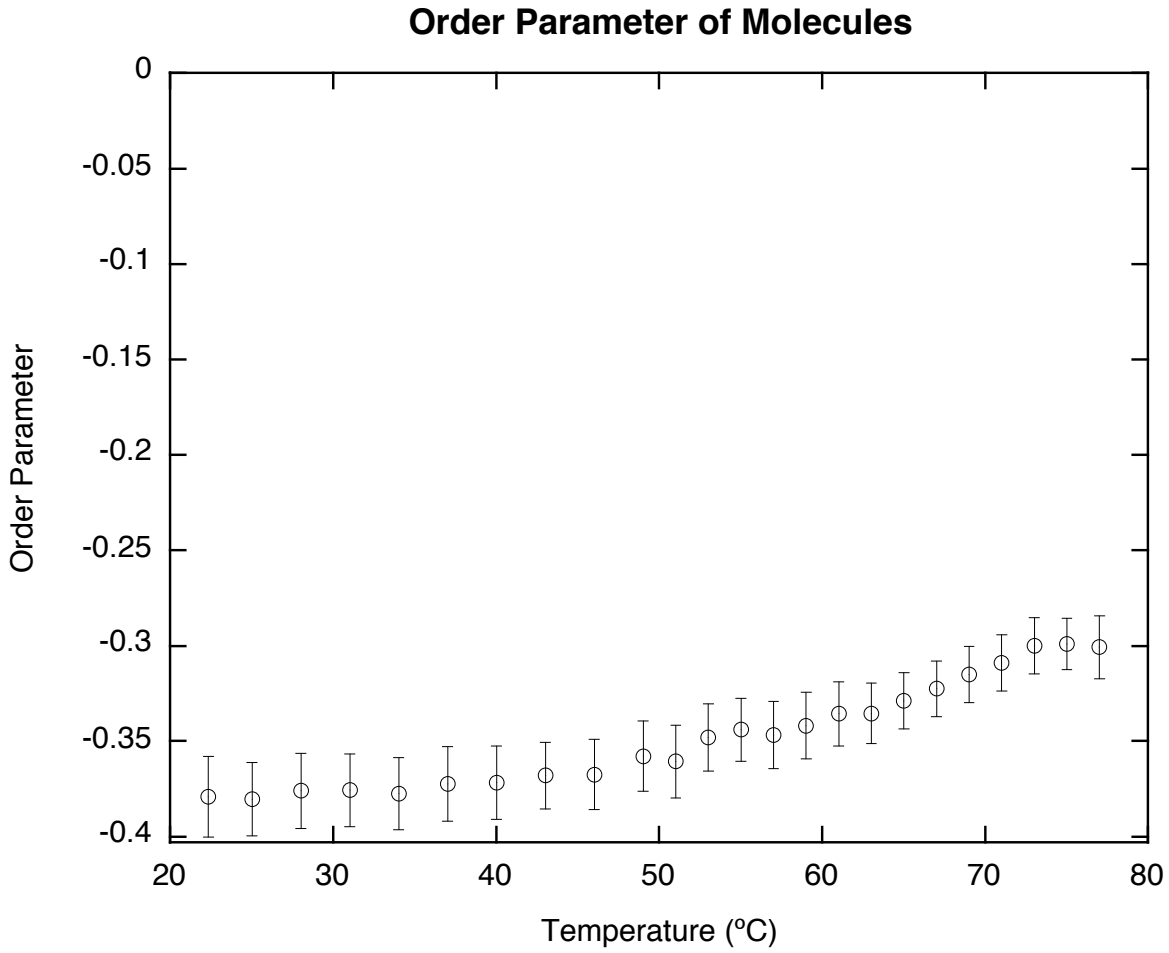

Figure 5.4: The order parameter S_{molec} of a sample of Sunset Yellow FCF, as it varies with temperature.

Chapter 6

Discussion

6.1 Model

Both the result of negative birefringence measurements, and the result of negative order parameter of the molecules independently suggest that the extraordinary index $n_e = n_\parallel$, where $n_\parallel$ is the index of refraction for light polarized parallel to the director, is the lower index of refraction by equations (4.1) and (2.28). For liquid crystals with a nitrogen-nitrogen double bond, the nitrogen-nitrogen double bonds dominate in the birefringence measurements. Similarly, the order parameter measurements were using absorption due to the nitrogen-nitrogen double bond. This can be understood qualitatively by considering the electron orbitals of the π bond between the two nitrogen atoms, as shown in Fig. 6.1. An electric field pointing parallel to the bond, such as the electric field of light polarized parallel to the bond, will accelerate the electron, whereas an electric field pointing perpendicular to the bond, such as that of light polarized perpendicular to the bond, will not be able to accelerate the electron as much, because the electron is unlikely to leave the orbital shown. Hence light polarized perpendicular to the bond will pass through with less interaction with the molecule than light polarized parallel to the bond, and the index of refraction $n_{\perp \mathrm{N=N}}$ for light polarized perpendicular to the nitrogen-nitrogen double bond is lower than the index $n_{\parallel \mathrm{N=N}}$ for light polarized parallel to the nitrogen-nitrogen double bond.

Therefore, the negative birefringence and the negative molecular order parameter each indicate that the nitrogen-nitrogen double bonds of the molecule are perpendicular to the long axis of the aggregate on average, as shown in Fig. 6.2. The figure shows the molecules all pointing in the same direction. X-ray measurements have shown that there is one molecule on each level of the stack [21]. The molecules are expected to lie flat in each level of the stack, but the molecules could be arranged in a number of ways.

The order parameter shown in Fig. 5.4 is S_{molec}, or equivalently $S_{\mathrm{N=N}}$, the order

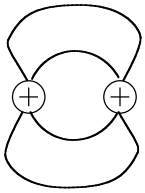

Figure 6.1: A π bond, as found between the two nitrogen atoms at the center of the Sunset Yellow FCF molecule. The nitrogen nuclei are shown with the electron cloud characteristic of a π bond. The double bond consists of two electrons, one in a σ bond (not shown) and one in a π bond. This second electron has the highest probability density of being observed in the areas shown. Note that the electron has greater freedom to move parallel to the bond than perpendicular to the bond. This influences its interactions with electromagnetic radiation polarized in this direction as explained in the text.

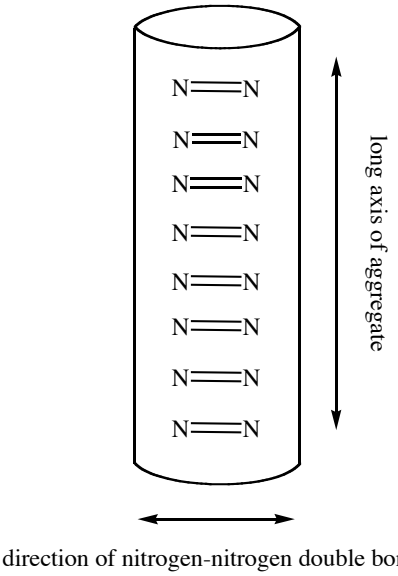

Figure 6.2: A model of aggregated molecules. The negative birefringence of aqueous Sunset Yellow is evidence for a general model where the molecules aggregate with the nitrogen-nitrogen double-bond of each molecule perpendicular to the long axis of the aggregate. Each molecule (see Fig. 3.1) is represented by its nitrogen-nitrogen double bond. It is not known what the orientation of the N=N bond within the horizontal plane.

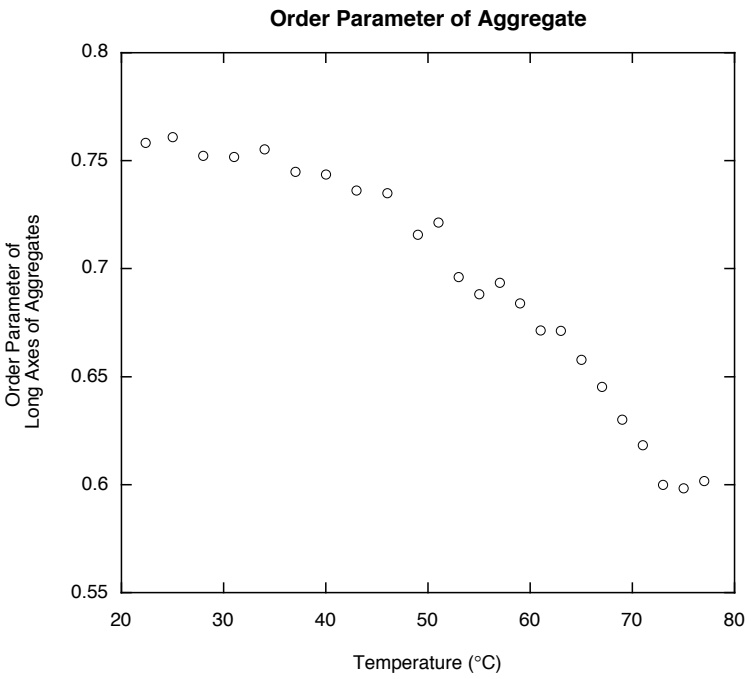

Figure 6.3: If I assume that the nitrogen-nitrogen double bonds are perpendicular to the long axis of the aggregate, as suggested by the model, then I can calculate the order parameter of the aggregate from the order parameter of the nitrogen-nitrogen double bonds.

parameter of the nitrogen-nitrogen double bonds, and thus of the molecules, rather than the order parameter S_{agg} of the elongated aggregates. Based on the model shown in Fig. 6.2, I assume that the angle between the aggregate long axis and the N=N bond of a molecule in the aggregate is $\theta_2 = 90°$. Then by Eq. (2.29), the order parameter of the aggregate is

$$S_{\text{agg}} = \frac{S_{\text{N=N}}}{P_2(\cos 90°)} = -2\, S_{\text{N=N}}. \tag{6.1}$$

This gives Fig. 6.3, the order parameter of the aggregate as a function of temperature. These values of the order parameter and dependence on temperature resemble what one finds in thermotropic liquid crystals.

6.2 Comparison of Experimental Results to Theoretical Phase Diagram

The theoretical phase diagram shown in Fig. 2.3 suggests that the slope of the transition curves should be 56°C/M for the isotropic-coexistence curve and 50°C/M for the coexistence-

nematic curve. The experimental results, shown in Fig. 5.1, show that the slopes are 177°C/M and 158°C/M, respectively. Hence the theory and the experiment disagree by a factor of 3 for the slope. The width of the coexistence region of the theoretical phase diagram is 25% larger than the width of the experimental phase diagram. The theoretical phase diagram and the experimental results agree that the slope of the isotropic-coexistence curve is higher than the slope of the coexistence-nematic curve. Given the simplicity of the theory, the fact that it applies to dilute solutions, and the fact that Onsager's result is for rods of a single length to width ratio, this shows that the basic behavior of the system is predicted with the most simple theory possible.

6.3 Work of others

6.3.1 Phase Diagram

Compared to the drug DSCG, Sunset Yellow undergoes a transition from the isotropic to the nematic phase at higher concentrations [7]. A comparison to Robert J. Luoma's dissertation [5] shows that the phase diagram I plotted agrees with previous measurements of Sunset Yellow FCF. The slope of the isotropic-coexistence curve in Fig. 5.1 is within 4% of the slope of Luoma's curve. In Fig. 5.1, the coexistence region occurs at approximately a 0.1 M higher concentration than Luoma's diagram. This is probably due to a different sample purity, water content of the solid, or amount of evaporation during filling.

6.3.2 Birefringence

Very recently, Shiyanovskii et al. [20] have reported that for DSCG, $\Delta n/(n_e + n_o) = -0.006$. For Sunset Yellow $\Delta n \sim -0.1$, $n_\parallel \approx 1.42$, and $n_\perp \approx 1.53$, so that $\Delta n/(n_e + n_o) \sim -0.03$. This suggests that the birefringence of Sunset Yellow is approximately 5 times that of DSCG.

6.3.3 Index of Refraction

Luoma measured the isotropic index of refraction with an Abbe refractometer and found $n_{\text{iso}} = 1.334 + 0.363\,\Phi$, where Φ is the volume fraction [5, p. 31]. Using Eq. (2.11) to convert from volume fraction to concentration, Luoma's result is approximately $n_{\text{iso}} = 1.334 + 0.117\,c$, where c is the concentration in molars. In Fig. 5.3, my results are $n_{\text{iso}} = 1.33 + 0.11\,c$. This slope differs by 5% from Luoma's slope, likely due to uncertainty in the concentration of the solutions.

6.3.4 Order Parameter

Hui and Labes [9] measured the order parameter of the bonds in DSCG and found values ranging from -0.071 to -0.149, depending on the bond measured. The order parameter of the N=N bond of Sunset Yellow, shown in Fig. 5.4, is approximately -0.35. If the molecules form a complicated structure and the bond in different molecules of DSCG makes lots of angles with the long aggregate axis, then it could lead to a small value as compared to the order parameter of Sunset Yellow's nitrogen-nitrogen double bond.

Goldfarb et al. [8] report that the order parameter of the aggregates of DSCG is quite high, but do not give specific values.

Chapter 7

Conclusions

I made some of the first fundamental measurements on an aggregated dye liquid crystal. The birefringence and order parameter measurements point to a model in which the nitrogen-nitrogen double bonds of the molecules are perpendicular to the long axis of the aggregate. Further research may show that other aggregated dye liquid crystals have similar or different structures.

Acknowledgments

I gratefully thank my thesis advisor, Professor Peter Collings, whose expertise and support made this possible. His invaluable advice and prompt feedback was incredibly helpful at every step of the way. I also acknowledge Swarthmore College, the University of Pennsylvania Laboratory for Research on the Structure of Matter, the National Science Foundation Research Experience for Undergraduates program, and the Surdna Foundation for their support of this work.

The faculty of the Department of Physics and Astronomy at Swarthmore College have been wonderful. Special thanks to Prof. Michael Brown for helping me with the statistical mechanics and Prof. Amy Bug for discussing wave mechanics with me.

I also thank Jerome Fung for editing the manuscript, Prof. Kathy Hirsch-Pasek for her enthusiasm and advice, Dina Aronzon for her apparatus diagrams and for understanding the theory before I did (and helping me along), Lauren Janowitz for her measurements of Sunset Yellow FCF, Laura Twichell for helping me revise the introduction, Eric Levy for programming the optical table with me, Cortland Setlow for his technical guidance and for reminding me to define my terms, B Daniel Fairchild for trying to find the analytic solution, Henry Garcia for making me clarify the difference between thermotropic calamitic liquid crystals and lyotropic chromonic liquid crystals, Marc Landeweer for discussing with me the attraction between two Sunset Yellow molecules, Prof. Robert Meyer for detailing some of Robert J. Luoma's measurements, and Aaron Modic for initial work on this project, including purifying the sample of Sunset Yellow.

Appendix A

Mathematica Calculations for the Statistical Mechanics of Aggregation

The following Mathematica program was helpful in the calculations of the Lagrange multiplier λ, the number of aggregates of i molecules per volume ν_i, and the average number of molecules in an aggregate $\langle n \rangle$ in section 2.1.1.

Set the concentration in Molars.

```
In[1]:= cm := 1.0
```

Set the temperature in degrees Celcius.

```
In[2]:= TC := 49.9
```

Now, with a concentration and a temperature, it is possible to calculate λ,ν_i, and <*n*> = avgn. First convert to convenient units: Kelvin and mol/m^3.

```
In[3]:= T = TC + 273.15
Out[3]= 323.05
In[4]:= c = cm * 1000
Out[4]= 1000.
In[5]:= Mw := 0.45238
In[6]:= ρ := 1400
```

In[7]:= $\Phi = \frac{Mw\, c}{Mw\, c + \rho}$

Out[7]= 0.244216

In[8]:= $b := 4.5 \times 10^{-28}$

In[9]:= $k := 1.38065 \times 10^{-23}$

In[10]:= $h := 6.62607 \times 10^{-34}$

In[11]:= $\epsilon := 8.67 \times 10^{-20}$

In[12]:= $y = \frac{\Phi\, e^{\epsilon/(k\,T)}}{b\,\left(\frac{2\,\pi\,\rho\,b\,k}{h^2}\right)^{3/2}\,T^{3/2}}$

Out[12]= 18.6256

As shown in Fig. 2.1, we wish to solve for *x*, given *y*. Mathematica's FindRoot function does this easily. For efficiency, the sum stops after i = 500; this is valid because *X* must be small so that the series converges for finite *y*.

In[13]:= $xx = \text{FindRoot}\left[y == \sum_{i=1}^{500} i^{5/2}\, X^i, \{X, .01, 0, 1\}\right]$

Out[13]= $\{X \to 0.54271\}$

In[14]:= x = (xx[[1]])[[2]]

Out[14]= 0.54271

The Lagrange multiplier λ is easily calculated from *x*.

In[15]:= $\lambda = \frac{\frac{\epsilon}{k\,T} - \text{Log}[x]}{b}$

Out[15]= 4.45551×10^{28}

In[16]:= mi[i_] := i ρ b

In[17]:= $\Lambda[i\_] := \frac{h}{\sqrt{2\,\pi\ mi[i]\,k\,T}}$

```
In[18]:= ν[i_] = Λ[i]^-3 ℯ^(-ϵ/(k T)) ℯ^(i (ϵ/(k T) - λ b))

Out[18]= 2.91374 × 10^25 ℯ^(-0.61118 i) i^(3/2)
```

The average number of molecules in an aggregate. For efficiency, the sum stops after i = 500; this is valid because the value of ν_i is very small for i > 500.

```
In[19]:= avgn = Φ / (b Σ_(i=1)^500 ν[i])

Out[19]= 4.11855
```

```
In[20]:= ListPlot[Table[{i, ν[i]}, {i, 0, 13, 1}],
           AxesLabel → {"i", "νi"}, PlotStyle -> PointSize[0.015]]
```

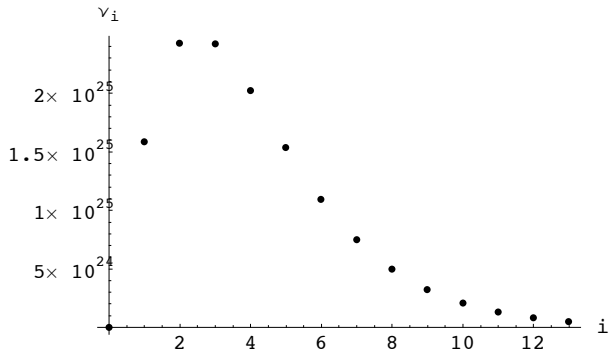


```
Out[20]= - Graphics -
```

This graph of ν_i versus i shows the distribution of aggregate lengths in an aqueous solution of Sunset Yellow FCF of this concentration and temperature.

```
In[21]:= avgn Φ

Out[21]= 1.00581
```

Appendix B

Rotating Matrices

If a vector **A** is represented by $\begin{bmatrix} A_x \\ A_y \end{bmatrix}$, then the Jones vector in a rotated frame is

$$\begin{bmatrix} A'_x \\ A'_y \end{bmatrix} = R(-\theta) \begin{bmatrix} A_x \\ A_y \end{bmatrix} = \begin{bmatrix} \cos\theta & -\sin\theta \\ \sin\theta & \cos\theta \end{bmatrix} \begin{bmatrix} A_x \\ A_y \end{bmatrix}.$$

Similarly,

$$\begin{bmatrix} B'_x & B'_y \end{bmatrix} = \begin{bmatrix} B_x & B_y \end{bmatrix} R^t(-\theta) = \begin{bmatrix} B_x & B_y \end{bmatrix} \begin{bmatrix} \cos\theta & \sin\theta \\ -\sin\theta & \cos\theta \end{bmatrix}.$$

So if a matrix M is formed by **A** and **B**,

$$M = \begin{bmatrix} A_x \\ A_y \end{bmatrix} \begin{bmatrix} B_x & B_y \end{bmatrix},$$

it will transform as

$$M' = R(-\theta)\, M\, R^t(-\theta)$$

where the rotation matrix is given by

$$R(-\theta) = \begin{bmatrix} \cos\theta & -\sin\theta \\ \sin\theta & \cos\theta \end{bmatrix}.$$

Appendix C

Details of the Procedure for Birefringence Measurements

The following provides the details for setting up the apparatus for birefringence measurements, shown in Fig. 4.5.

I screwed polarizer B onto the rotating microscope stage, and rotated it so that it was crossed with polarizer A above the microscope stage. Then I fixed polarizer B in place by tightening a screw on the microscope stage. I placed the heating stage containing the sample of Sunset Yellow on polarizer B on the microscope stage. I positioned the heating stage so that the director of the liquid crystal sample was parallel to polarizer B, verifying that the light passing through polarizer B, the sample, then polarizer A was extinguished with the heating stage at this angle. I placed a quarter wave plate on top of the heating stage, and aligned the fast axis with polarizer B. As before, the light passing through was extinguished.

I rotated the heating stage 45° to the right. Because I had chosen this particular region of the cell, I assured that the heating stage didn't drift too far to the side during rotation by resting my fingers on the microscope stage as I turned the heating stage, and watching the sample through the microscope while rotating. Then I taped the heating stage onto polarizer B. The quarter wave plate had rotated with the heating stage, and I rotated it 45° to the left so that it was parallel with polarizer B as before.

Now polarizer B was crossed with polarizer A, the director in the sample was rotated 45° to the right from polarizer B, and the fast axis of the quarter wave plate was parallel with polarizer B. I untightened the screw holding the microscope stage and polarizer B so that it could rotate freely. The heating stage and the quarter wave plate rotated with polarizer B, while polarizer A remained fixed.

I placed a 633-nm filter over the light source, and turned off the lights in the room

to minimize other sources of light. I rotated the microscope stage along with polarizer B, the sample in the heating stage, and the quarter wave plate, and I observed the angle α where the light intensity was lowest on an oscilloscope measuring the output from the light detector. Since it was difficult to identify the exact angle that minimized the light intensity, I would rotate the stage to two angles on either side of α that had the same light intensity and I would take the average of those two angles to find a value for α. I would then repeat this with two other angles on either side of α, and both averaged values for α were used.

Bibliography

[1] P. J. Collings and M. Hird. *Introduction to Liquid Crystals: Chemistry and Physics*. Taylor & Francis, Bristol, PA, 1997.

[2] J. E. Lydon. Chromonic liquid crystal phases. *Current Opinion in Colloid & Interface Science*, 1998(3):458–466, 1998.

[3] P. K. Maiti, Y. Lansac, M. A. Glaser, and N. A. Clark. Isodesmic self-assembly in lyotropic chromonic systems. *Liquid Crystals*, 29(5):619–626, 2002.

[4] J. E. Lydon. Chromonics. In D. Demus, J. Goodby, G. W. Gray, H.-W.Spiess, and V. Vill, editors, *Handbook of Liquid Crystals*, volume 2B, chapter XVIII, pages 981–1007. Willey-VCH, New York, 1998.

[5] R. J. Luoma. *X-ray scattering and magnetic birefringence studies of aqueous solutions of chromonic molecular aggregates*. PhD thesis, Brandeis University, 1995.

[6] J. S. Cox, G. D. Woodard, and W. C. McCrone. Solid-state chemistry of cromolyn sodium (disodium cromoglycate). *J. Pharm. Sci.*, 60(10):1458–65, 1971.

[7] N. H. Hartshorne and G. D. Woodard. Mesomophism in the system disodium chromoglycate-water. *Molecular Crystals and Liquid Crystals*, 23:343–368, 1973.

[8] D. Goldfarb, Z. Luz, N. Spielberg, and H. Zimmermann. Structural and orientational characteristics of the disodium/cromoglycate-water mesophases by deuterium nmr and x-ray diffraction. *Mol. Cryst. Liq. Cryst.*, 126:225–246, 1985.

[9] Y. W. Hui and M. M. Labes. Structure and order parameter of a nematic lyotropic liquid crystal studied by ftir spectroscopy. *J. Phys. Chem.*, 1986(90):4064–4067, 1986.

[10] D. Perahia, D. Goldfarb, and Z. Luz. Sodium-23 NMR in the lyomesophases of disodiumcromoglycate. *Mol. Cryst. Liq. Cryst.*, 108:107–123, 1984.

[11] J. E. Turner. *Lyotropic discotic dye/water systems.* PhD thesis, University of Leeds, 1988.

[12] J. E. Turner and J. E. Lydon. Chromonic mesomorphism: The range of lyotropic discotic phases. *Mol. Cryst. Liq. Cryst. Letters*, 5(3):93–99, 1988.

[13] D. Perahia, Z. Luz, and E. J. Wachtel. N.M.R. and X-ray diffraction of the 7,7'-disodiumcromoglycate-water lyomesophases. *Liquid Crystals*, 2(4):473–489, 1987.

[14] D. Perahia, E. J. Wachtel, and Z. Luz. NMR and X-ray studies of the chromonic lyomesophases formed by some xanthone derivatives. *Liquid Crystals*, 9(4):479–492, 1991.

[15] G. J. T. Tiddy, D. L. Mateer, A. P. Ormerod, W. J. Harrison, and D. J. Edwards. Highly ordered aggregates in dilute dye-water systems. *Langmuir*, 1995(11):390–393, 1995.

[16] C. Ruslim, D. Matsunaga, M. Hashimoto, T. Tamaki, and K. Ichimura. Structural characteristics of the chromonic mesophases of C.I. Direct Blue 67. *Langmuir*, 2003(19):3686–3691, 2003.

[17] T. Schneider, A. Smith, and O. D. Lavrentovich. Imaging oriented aggregates of lyotropic chromonic mesogenic dyes by atomic force microscopy. *Mat. Res. Soc. Symp.*, 636:D11.8.1–D11.8.5, 2001.

[18] H. Stegemeyer and F. Stöckel. Anisotropic structures in aqueous solutions of aggregated pseudoisocyanine dyes. *Ber. Bunsenges. Phys. Chem.*, 100(1):9–14, 1996.

[19] K. Ichimura, T. Fujiwara, M. Momose, and D. Matsunaga. Surface-assisted photoalignment control of lyotropic liquid crystals. Part I. Characterisation and photoalignment of aqueous solutions of a water-soluble dye as lyotropic liquid crystals. *J. Mater. Chem.*, 2002(12):3380–3386, 2002.

[20] S. V. Shiyanovskii, T. Schneider, I. I. Smalyukh, T. Ishikawa, G. D. Niehaus, and K. J. Doane. Real-time microbe detection based on director distortions around growing immune complexes in lyotropic chromonic liquid crystals. *Phys. Rev. E*, 71(2):020702-1–020702–4, 2005.

[21] P. J. Collings. Personal communication, Fall 2004 - Spring 2005.

[22] L. Janowitz. Personal communication, Spring 2004.

[23] F. Reif. *Fundamentals of Statistical and Thermal Physics*. McGraw-Hill, New York, 1965.

[24] P. G. de Gennes. *The Physics of Liquid Crystals*, chapter 2.2.1.1, pages 34–39. Clarendon Press, London, 1974.

[25] David J. Griffiths. *Introduction to Electrodynamics*. Prentice Hall, Upper Saddle River, NJ, third edition, 1999.

[26] B. E. A. Saleh and M. C. Teich. *Fundamentals of Photonics*, chapter 5.5.A, pages 174–176. John Wiley & Sons, Inc., New York, 1991.

[27] G. B. Arfken and H. J. Weber. *Mathematical Methods for Physics*. Academic Press, San Diego, fourth edition, 1995.

[28] F. L. Pedrotti and L. S. Pedrotti. *Introduction to Optics*, chapter 14, pages 280–297. Prentice Hall, Upper Saddle River, NJ, second edition, 1993.